KfK 3987
EUR 10391EN
Mai 1986

Resuspension of Fission Products during Severe Accidents in Light-Water Reactors

R. Borkowski, H. Bunz, W. Schöck
Laboratorium für Aerosolphysik und Filtertechnik

Kernforschungszentrum Karlsruhe

KERNFORSCHUNGSZENTRUM KARLSRUHE
Laboratorium für Aerosolphysik und Filtertechnik

KfK 3987
EUR 10391 EN

RESUSPENSION OF FISSION PRODUCTS DURING SEVERE ACCIDENTS IN LIGHT-WATER REACTORS

R. Borkowski, H. Bunz and W. Schöck

Kernforschungszentrum Karlsruhe GmbH, Karlsruhe

Als Manuskript vervielfältigt
Für diesen Bericht behalten wir uns alle Rechte vor

Kernforschungszentrum Karlsruhe GmbH
Postfach 3640, 7500 Karlsruhe 1

ISSN 0303-4003

Resuspension of fission products during severe accidents in light water reactors

Abstract

This report investigates the influence of resuspension phenomena on the overall radiological source term of core melt accidents in a pressurized water reactor. A review of the existing literature is given and the literature data are applied to calculations of the source term. A large scatter in the existing data was found. Depending on the scenario and on the data set chosen for the calculations the relative influence of resuspended fission products on the source term ranges from dominant to negligible.

The work was supported by the Commission of the European Communities under study contract ECI-1077-B7221-83-D.

Resuspension von Spaltprodukten aus dem Sumpf bei schweren Unfällen in Leichtwasserreaktoren

Zusammenfassung

In diesem Bericht wird der Einfluß der Resuspension auf den radiologischen Quellterm bei Kernschmelzunfällen in Druckwasserreaktoren untersucht. Es wurde eine Literaturrecherche durchgeführt und deren Ergebnisse in Quelltermrechnungen verwendet. Die Streubreite der Literaturdaten ist beträchtlich. In Abhängigkeit vom Scenario und davon, welche Daten verwendet werden, ergibt sich, daß der relative Einfluß der Resuspension auf den Quellterm von 'dominierend' bis 'vernachlässigbar' reicht.

Diese Arbeit wurde von der EG-Kommission im Rahmen des Studienvertrags ECI-1077-B7221-83-D unterstützt.

Contents

Introduction

Fission-product behaviour during core meltdown accidents has been a central part of the risk studies which have been conducted in the USA and the Federal Republic of Germany (1,2) and was recently the subject of a special study by a group of experts (3).
According to these studies, the fission products are released from the nuclear fuel to the primary system and the reactor containment in different phases during an accident. Depending on the availability of safety features, some of the airborne fission products enter the environment and cause damage to health and property.

For convenience, the main fission products are divided into three groups of comparable activity but different behaviour:

(I) Noble gases, which are released in their entirety from the overheated core and are considered to enter the environment in large quantities because of the lack of possible retention mechanisms.

(II) Halides, chiefly iodine, which are also very volatile but of great chemical reactivity and subject to considerable retention in the reactor building, an important exeption being organic iodides.
Retention is due to the formation of water-soluble inorganic compounds which are likely to be retained in the containment sump formed by main and auxiliary primary circuit coolant during the accident. A recent study of this is to be found in (4).

(III) Aerosols containing fission products of lower volatility such as Cs, Se, Te, Sb, Sr, Ru, activation products and transuranic elements are removed from the containment atmosphere by aerosol processes and considered to be trapped in the building sump and on wet surfaces, thus being retained in significant quantities in the reactor building. The role of aerosols in core melt accidents has recently been examined in (5, 6, 7).

Since more is now known about the retention mechanism, post-WASH-1400 evaluations of fission product behaviour tend to assume lower releases of fission products to the environment than the conservative values given by studies (1) and (2), in view of this, more importance

has to be attached to some phenomena which used to be considered of minor significance. One of these is the problem of the amount of fission products in the containment sump that could be revolatilized to the building's atmosphere, thus constituting a low-level but long-lasting source of radioactivity. Once the sump is dried, additional release from the residue might occur. The possibility of resuspension of fission products on depressurization of the reactor containment is hinted at in (5). Another reference to the general possibility of resuspension is to be found in (8).

This study looks at what is known and what further work is required on fission product resuspension from the containment sump during severe accidents. Its prime concern is aerosol resuspension, but because of the important role of fission products dissolved in water attention is also given to revolatilization of dissolved matter by aerosol formation. Fission product noble gases are not dealt with.

The first four chapters summarize the information contained in the literature from different points of view. The first two chapters describe the results of experiments with the two distinct types of revolatilization of solubles and particles from liquids. In chapter 3 the information available on the release mechanism and on the influence parameters is given. Most of this chapter deals with revolatilization of solubles by entrainment from boiling liquids, which is the easiest way to study the phenomenon. The mathematical model is briefly described in chapter 4.

Chapter 5 contains an evaluation of the existing data as regards their applicability to the core melt scenario. In chapter 6 the results of aerosol behaviour calculations are presented. These calculations were done using the NAUA code for calculating aerosol behaviour in LWR accidents in this study in order to assess the influence of revolatilization mechanism on the radiological source term. The calculations show that revolatilization processes are clearly

a significant component of the radiological source term, but also that the uncertainty is considerable. For this reason chapter 7 points out what information is lacking and makes suggestions for further research.

1. Resuspension of solid particles from pools

The term 'resuspension' shall be understood here as the transition of solid particles from suspension in a bulk liquid to airborne suspension above the surface of the bulk liquid. 'Re-entrainment', on the other hand, is used to describe the formation of liquid solution droplets above a bulk liquid solution by mechanical disintegration of the surface of that solution.

In connection with the sodium tests described below, Sauter and Schütz (14, 15) made explorative experiments on the release of sand and dyes from an evaporating water pool. The experimental setup is shown in Figure 1. Temperatures were below boiling point and the particle size of the sand was less than 50 µm. The covering air was slowly driven through a particle filter and a cold trap. The sand released was collected on the filter and the evaporated water was condensed in the cold trap. Both were weighed to permit a rough calculation of the retention factors. Values of 1000 were obtained at just below boiling point and 4×10^4 at a temperature somewhat lower. No release at room temperature was measurable. From personal communication from the authors it is known that during these experiments about 10 % of the liquid was evaporated and the water used had been degassed prior to the experiment. Similar experiments were conducted with suspensions and solutions of different dyes in water. In the case of these the effect was confirmed but not quantified.

J. A. Quinn et al. (16) have investigated particle transfer to drops produced by the bursting of 1 mm bubbles at an aqueous surface. The particles used in the experiments were polystyrene latex spheres 0.48 and 0.79 µm in diameter, which were suspended in KCl solutions of varied ionic strength. Different latex particle concentrations between 10^6 and $10^{10}/cm^3$ and different bubble release depths were used. The experiments were conducted at room temperature. The simple apparatus for bubble generation and drop collection is shown in Figure 2. The drops were collected on a microscope slide and the particles optically counted. Particle concentration in the collected drops was found to be basically independent of particle concentration in the bulk liquid and this

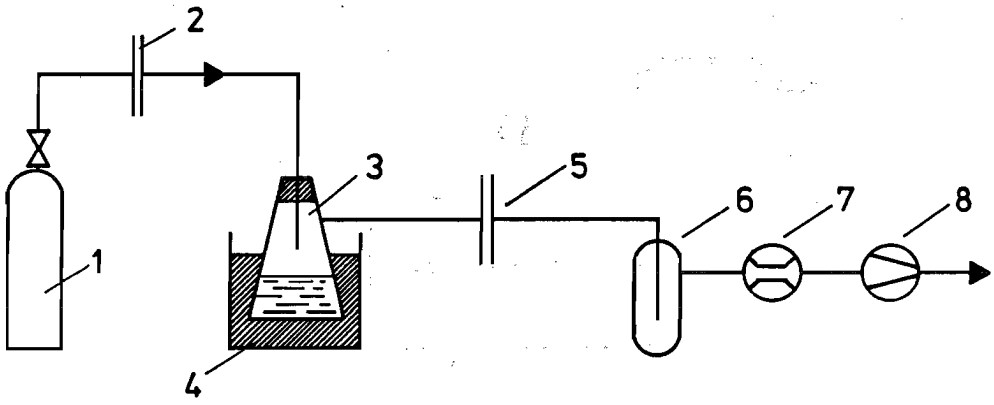

Figure 1 Experimental setup of the water-sand experiments (14)

1 - pressurized air
2,5 - filters
3 - container with mixture of 600cm³ of water and 100g of sand
6 - cold trap (condenser)
7 - flow meter
8 - pump

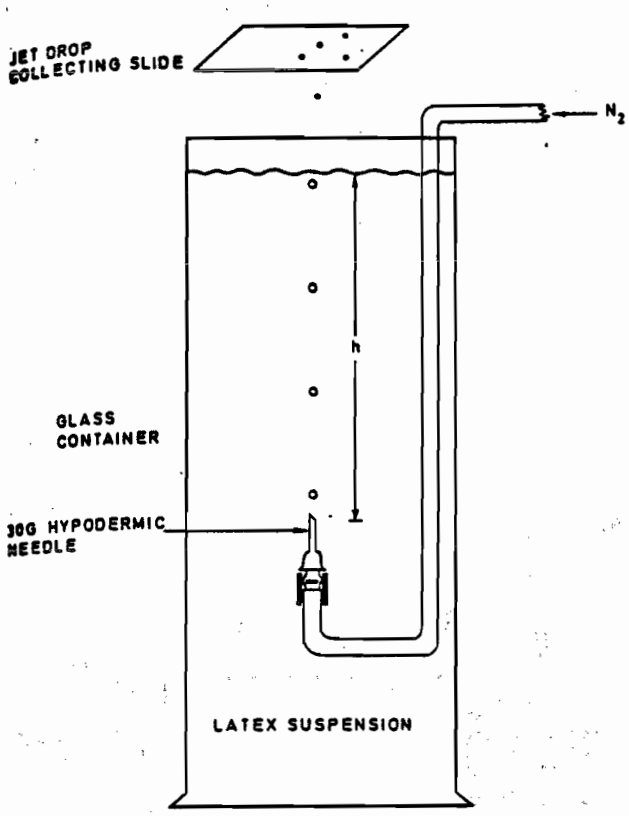

Figure 2 Bubbling apparatus used by (16)

was attributed to the fact that the surface was saturated with particles. Drop concentration increased with release depth (or bubble age) and ionic strength.
The results were discussed by the author but no clear explanation was found.

W. J. Marble et al. (17) investigated retention of fission product aerosols by BWR suppression pools during reactor accidents. In order to test related theoretical models, a series of scrubbing experiments were performed. In the experiments nitrogen was charged with oxide particles of the density and size distribution conceivable in reactor accidents and scrubbed by means of a water bath of varied depth. The different parameters tested and the experimental setup are reproduced in Fig. 3.
Decontamination factors were determined by comparing the quantity of oxide collected in the tank water and in the backup sampler, and were found to lie between 100 and 4×10^3, depending on the bubble residence time and particle size. Bubble size and temperature were of no influence. A summary of test results is given in Table 4.

The process which is the subject of these experiments is essentially the inverse of the one we want to know more about. But assuming that an equilibrium has been reached between the processes of absorption and desorption of particles in the pool we may consider the reported decontamination factor as the inverse of the release fraction. The release fraction calculated from the reported D.F.'s will range from 10^{-2} to 2.5×10^{-4}. Despite its somewhat speculative character owing to the uncertainty of equilibrium, the range of values found is of the same order to magnitude as that reported by other authors cited in this chapter.

The suppression pool scrubbing effect was examined by (61) in 1981. From this report it can be seen that Marble's results are in general confirmed by the work of other authors. The decontamination effect of a 2040 gal. scale model of a subcooled pool on 0.06µm nickel-chromium aerosol carried by air-steam mixtures was a D.F. of 49 to 841 (62). Small-scale laboratory tests and larger-scale tests with a 150 gal. scrubbing pool at a temperature of 50°C yielded D.F. values of 50 to 100 using 0.06 µm nickel-chromium aerosols in steam-air mixtures (63).

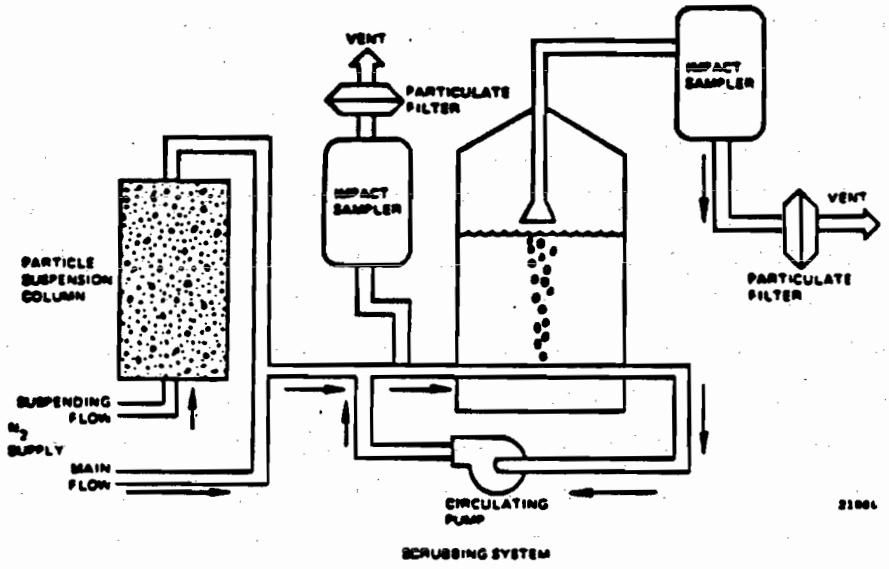

PARAMETERS TESTED

- **Bubble Size** — **0.4 — 1.4 CM**
- **Particle Concentration:** — **0.02 — 5.5 G/M^3**
- **Submergence Height:** — **34 — 167 CM**
- **Gas and Water Temperature:** — **20°C and 60°C**
- **Particle Size Distribution:** — **0.05 to 10 μM**

Figure 3 Particulate scrubbing experiments (17)

Table 4: Scrubbing test results (17)

SUMMARY OF SCRUBBING TEST RESULTS

Test Number	Bubble Diam, cm	Orifice/ Cap	Bubble Rate B/M	Particle Conc (g/m^3)	Water Height (cm)	Overall D.F.
1	0.47	70/none	183	0.18	34.3	108
2	0.63	70/0.6	145	0.17	34.3	333
3	0.63	70/0.6	145	0.44	34.3	214
4	0.60	70/0.6	277	0.02	34.3	119
5	0.74	130/0.8	254	0.53	34.3	189
6	0.85	180/0.8	312	0.48	167.7	1170
7	0.85	180/0.8	318	0.91	167.7	1415
8	0.45	180/0.2	248	0.87	167.7	1251
9	0.45	180/0.2	48	0.48	167.7	719
10	0.86	180/0.7	260	0.76	167.7	896
11	0.86	180/0.7	260	5.5	167.7	1260
12	1.41	Special	124	0.30	167.7	534
13	1.35	Special	140	1.8	167.7	1260
14	0.78	180/0.7	248	4.95	76.2	910
15	0.88	240/0.7	276	4.34	167.7	4157
16	0.88*	240/0.7	272	1.38	167.7	2270
17	0.88	240/0.7	304	**N.D.	167.7	928

* 60 C Water/60 C Gas
** Not Determined

Jordan, Ozawa, Sauter and Schütz (14,15,18-21) have reported experiments on the release of sodium, fuel and simulated fission products from hot and boiling sodium pools. The results are summarized in (14) and (15). The experimental program was divided into two phases with laboratory-scale (I) and full-scale (II) experiments. In addition laboratory-scale experiments with aqueous systems were conducted which are reported above.

I. The small-scale sodium experiments were conducted in three different types of stainless steel containers - sketched in Figure 5 - with an approx. volume of 500 cm^3 under an inert gas atmosphere of controlled flow and different flow patterns. The material released by this flow was transported to filters which were analyzed with respect to sodium and uranium by chemical titration and fluorometry. The amount of sodium was of the order of 100 g and the added UO_2 of the order of a few g. The area of the melt surface was 38.5 cm^2. Typical evaporation from the mixture during the experiments was 10 %. The residue in the pool was analyzed for its UO_2 content and the size distribution of the fuel powder remaining.

Temperatures, concentrations and mean particle size of the fuel powder in the sodium, inert gas flows and sodium pool geometries were varied and the results presented in terms of retention factors which are defined as the ratio of mass concentration of uranium in the pool to the mass concentration in the released aerosol. The experimental results are compiled in Table 6a)to d). Retention factors were generally of the order of 1000 even under boiling conditions. Experiments with free convection at the sodium surface, summarized in Table 6 d), showed somewhat lower release. Release of uranium was experimentally proven to be (at least in part) in the form of particulates with mean diameter smaller than that of the original UO_2 powder.

Post -experimental uranium analysis of the sodium residue in separate horizontal layers showed marked enrichment of particles containing uranium at the surface with particle size distribution there similar to that

found on the filtered aerosol. This was also shown to exist during the experiments, by liquid sampling at varied depth. The surface enrichment - shown in Figure 7 - is considered to be an important link in the release mechanism. In the experiments with forced gas convection parallel to the phase interface the surface fraction of the particles and the released fraction were both considerably higher, which was attributed to enhanced convection in the sodium. The authors consider this convection to be transportational link between the bottom layer of uranium and the enriched layer at the surface and as such decisive for the release.

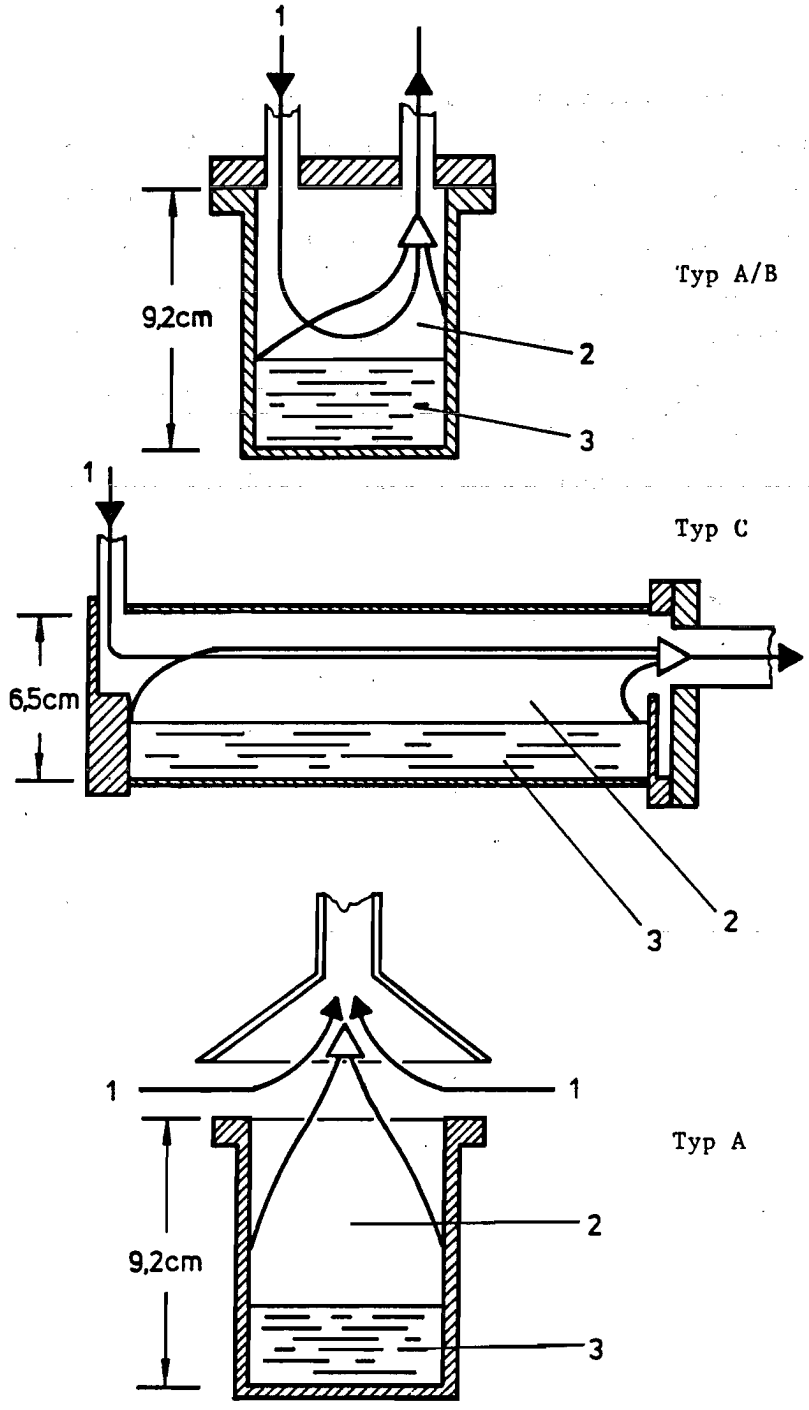

Figure 5 Sodium containers and gas flow pattern used by (14)

1 - gas flow

2 - aerosol

3 - sodium pool

Table 6 Experimental results obtained and compiled by (14)

t - duration of the experiment
v - gas flow
Na frei - released sodium
U frei - released uranium
RF - retention factor
$\bar{d}$ - mean particle size of the UO_2 powder

a) experiments using 20µm powder of UO_2 and type A and B containers

Exp. Nr.	T [°C]	Na [g]	UO_2 [g]	t [min]	v [l/min]	Na frei [g]	U frei [µg]	RF
1	892	100	8,48	6	0	40,0	1580	$2,0 \cdot 10^3$
2	892	100	8,68	6	0	23,9	1230	$1,4 \cdot 10^3$
3	892	100	0,76	2	0,6	45,0	394	$1,1 \cdot 10^3$
4	530	100	0,84	87	17	12,3	42	$2,1 \cdot 10^3$
5	530	100	0,72	93	10	2,0	5	$2,5 \cdot 10^3$
6	530	100	0,95	60	1	0,9	4	$1,8 \cdot 10^3$
7	530	100	10,25	60	10	2,8	104	$2,5 \cdot 10^3$
8	437	51	1,17	120	1	0,2	1	$0,8 \cdot 10^3$
9	723	50	1,27	17	1	6,9	243	$0,7 \cdot 10^3$
10	814	56	1,88	9	1	20,1	300	$2,0 \cdot 10^3$
11	700	101	2,46	10	5	4,6	109	$0,9 \cdot 10^3$

b) experiments using UO_2 powders of varied particle size

Exp. Nr.	UO_2 [g]	$\bar{d}$ [µm]	Na [g]	T [°C]	t [min]	v [l/min]	Na frei [g]	U frei [µg]	RF
12	2,00	112	98	700	10	5	4,1	94	$0,9 \cdot 10^3$
13	2,20	188	102	700	15	5	8,2	236	$0,7 \cdot 10^3$
14	2,36	565	102	700	15	10	12,1	39	$6,3 \cdot 10^3$
15	5,00	Pellets	108	620	20	15	9,5	< 2	$> 2 \cdot 10^5$
16	5,28	Pellets	94	720	75	0,5	4,5	< 1	$> 2 \cdot 10^5$
17	5,30	Pellets	52	825	20	0,5	36,4	< 7	$> 4 \cdot 10^5$

Table 6 (continued)

c) experiments with gas flow parallel to the sodium surface (type C container)

Exp. Nr.	T [°C]	Na [g]	UO_2 [g]	$\bar{d}$ [µm]	t [min]	v [l/min]	Na frei [g]	U frei [µg]	RF
18	623	178	1,41	20	15	20	11,2	1744	45
19	530	150	0,95	20	90	7,5	5,1	1083	26
20	623	164	8,35	20	20	14	7,1	7118	45
21	623	151	2,45	188	20	8,6	7,3	74	$1,4 \cdot 10^3$

d) experiments with free convection at the sodium surface

Exp. Nr.	T [°C]	Na [g]	UO_2 [g]	$\bar{d}$ [µm]	t [min]	v [l/min]	Na frei [g]	U frei [µg]	RF
22	520	103	1,90	20	90	--	4,25	12	$6,0 \cdot 10^3$
23	485	102	2,00	20	75	--	2,64	22	$2,1 \cdot 10^3$
24	510	103	11,0	188	90	--	4,91	14	$3,3 \cdot 10^4$

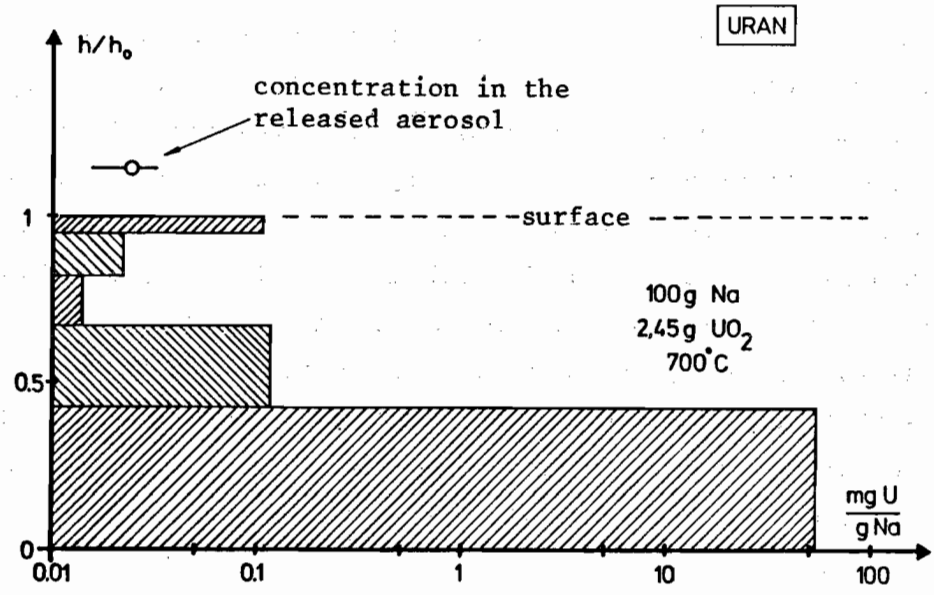

Figure 7 Uranium concentration measured by (14) in the sodium pool at different relative depths

Further experiments were conducted with regard to the time behaviour of uranium release. High initial release was found to decrease strongly with time. Because of this, integral release at complete vaporiation was shown by experiments not to exceed the values given above for 10 % vaporization. Other than from gas flow, no significant influence of the various experimental parameters was found.

II. Larger experiments (15) were conducted with approx. 1 kg of sodium melt with a surface area of 531 cm^3. Because the major interest was in aerosol phenomena, the container had a volume of 2.2 m^3 and natural gas-phase convection only. The inert cover gas was at atmospheric pressure. The evaporated sodium fraction was about 10 % and the pool temperature approximately 550°C. During the experiments aerosol samples were drawn through a bubbler and the resulting solution and solutions obtained by post-experimental washing of the wall and of deposition coupons were analyzed for sodium and uranium content. The sodium residue was analyzed as well. Experiments conducted with UO_2 particles of 10 and 20 µm mean size confirmed the retention factors obtained by small-scale experiments. The retention of 200 µm particles was at the detection limit of $2x10^4$. The experimental conditions and results are shown in Table 8.

M. Berlin et al.(9) evaluated in addition the retention of fission products and nuclear fuel by liquid and boiling sodium. In the experiments 4 to 5 kg of sodium was heated to temperatures approaching and at boiling point and completely evaporated. The sodium was doped with powders of UO_2 or fission product oxides of different mean particle sizes between 1.2 and 200 µm. The evaporating pan was installed in a 4.6 m^3 steel container filled with nitrogen. During the experiments filter samples were drawn from the atmosphere and afterwards the vessel was washed with water or steam and the washing-water analyzed. From the content of uranium in the washings and filter samples retention factors were determined. The results are shown in Table 9. In one experiment (PAVE 4) the evaporation residue was analyzed for particle size distribution. Fractionation of the initial 200 µm powder to a few µm was found. The retention factors obtained were in the region of 1000 in experiments conducted at temperatures near to 800°C.

Table 8 Experimental conditions and results of (15)

a) particle size and results

Exp. Nr.	particle size $\langle \mu m \rangle$	retention factor RF	detection limit RF
T 5	200	$19{,}0 \cdot 10^3$	$20 \cdot 10^3$
T 6	20	$1{,}5 \cdot 10^3$	$20 \cdot 10^3$
T 7	20	$8{,}2 \cdot 10^3$	$40 \cdot 10^3$

b) temperatures and evaporation rates

Experiment	$\langle T \rangle$ (°C)	$\langle \dot{m} \rangle$ ($kg/m^2 \cdot h$)
T 6	550	0,798
T 7	557	1,026
T 5	564	1,526

Table 9 Results and experimental conditions of the sodium experiments of (9)

EXPERIENCES	TEMPERATURE	QUANTITE DE SODIUM	COMPOSES RADIOACTIFS DANS LE SODIUM			FACTEURS DE RETENTION MOYENS
			Nature	Taille moyenne	Quantité	
PAVE 2	800°C	4,6 kg	UO_2	2 m	60 g	950
PAVE 3	780°C	4,4 kg	UO_2	10 m	126 g	2 000
PAVE 4	780°C	4,4 kg	UO_2	200 m	95 g	1 100
PAVE 5	Boiling	4,4 kg	UO_2	2 m	148 g	60
PAVE 6	Boiling	4,9 kg	^{85}SrO	1,8 m	0,2g (120 Ci)	300
			$^{141}CeO2$	1,2 m	1,2g (259 Ci)	100
			^{103}Ru	2,4 m	0,7g (58 Ci)	180
PAVE 7	Boiling	5 kg	UO_2	2 m	271 g	80

and of the order of 100 at boiling temperature. The latter values are lower than those in (14,15) and probably result from the perturbations caused by boiling. The mean particle size of the UO_2 additive showed no clear influence on the retention. The authors suppose that the fraction released originates from a fraction of very fine particles which was present in all powders.

To summarize the information from the literature as given above, it can be seen that little is known about the central topic of particle resuspension from aqueous systems. The order of magnitude of the released fraction as obtained from exploratory experiments and indirect information is approximately 10^{-3}. Key parameters influencing the release are not known. For example, even temperature dependence is not clearly established. For temperatures above the boiling point the idea is supported by experiment that bubble-induced droplet formation might be a possible mechanism for liquid aerosol generation and particle resuspension. Below the boiling point no mechanism is known.

The results in the case of sodium suggest - in part - possible influence of surface effects on the release and show on a broader experimental base the same order of magnitude as those for water. However, density, surface tension, and contact angles of sodium systems are different from the corresponding values of aqueous systems. The enhanced surface tension of sodium systems may lead to an increased surface enrichment and release of particles. It cannot, therefore, be taken for granted that these results can be transferred to reactor sumps.

2. Re-entrainment of dissolved matter

This chapter summarizes the results of experiments on the volatilization of droplets and dissolved matter from evaporating or bubbling aqueous solutions. This phenomenon of volatilization is called entrainment, the term used in the context of industrial processes of evaporation and other separation methods. Outside this field a lot of information has been obtained from nuclear safety research. Similar information has also been gathered from liquid spills (25), liquid sludge application to land (26) and cooling-tower operation (27), but is not referred to here in detail because the mechanisms involved are less relevant.

When considering the values given for 'entrainment', 'carry-over' and so on it is important to be cautious of differences between static experiments with constant conditions (for example, solute concentrations), and non-static ones, as in the case of complete evaporation. The reported values of entrainment are often expressed as ppm liquid in the vapour. Values presented as $\mu g/m^3$ are roughly the same as ppb values since around atmospheric pressure 1 m^3 of common gases weighs approximately 1 kg. Another consideration is whether the amount of liquid or its content of solids has been measured.

J. Mishima et al. (28) studied plutonium release from evaporating aqueous plutonium nitrate solutions. Two areas studied by the authors are of interest in this chapter:

(I) aerosol release during the air drying of shallow pools of concentrated plutonium nitrate solution,

(II) aerosol release during evaporation of pools of plutonium nitrate solution with varied heat inputs.

(I) In the apparatus shown in Figure 10 small volumes (2-3 ml) of concentrated plutonium nitrate solution were air dried with and without heating by passing air at low velocities across the surface of the liquid. The liquid was held in a stainless steel dish 1 - 1.5 " in diameter. This dish was positioned by a Teflon holder in a Pyrex containment

vessel. The atmosphere was exchanged during the experiments by a filtered and controlled air flow drawn through a condenser and a membrane filter. After the heating cycle the filters were examined microscopically and filters, condensate and containment was radiometrically analyzed for plutonium content. Experimental data and results are compiled in Table 11, supplied by the authors. In most cases, the major part of the released material was retained in the containment. This amount was at the most $2\text{-}2.7 \times 10^{-4}$ of the plutonium inventory. Released fraction collected on the filter during evaporation was of the order of 10^{-5} at boiling conditions. Condensate fraction was below 10^{-4}. In spite of data scatter an increase of the released amount with increased temperature is clearly seen. No marked dependence on air velocity was observed.

(II) Further investigations were conducted by evaporating a pool of 100 cm^3 containing plutonium nitrate. The liquid was held by a 180 cm^3 glass beaker, which was heated from the side and bottom. The vapour rising from the beaker was collected in a 4 dm^3 pyrex jug. Steam and - in most experiments - air was drawn through this, passing a glass-fibre filter, a condenser, and an additional back-up filter. The apparatus is shown in Figure 12. The solution was quickly heated to the desired temperature and 90 % was boiled off. Boiling regimes were classified by degree of surface disturbance into "simmering", "disturbed surface" and "boiling" and further characterized by average boil-off rates. Temperatures of the solutions are not given. Air-flow and Pu-concentration were essentially constant. Plutonium collected by the first filter is designated as "airborne", desposits on wall and bottom of the Pyrex hood as "fall-out". In some cases, the top filter was changed after a period needed to evaporate 30 cm^3 in order to obtain information about the concentration effect on release. Experimental data and results are shown in Table 13. Plutonium fraction exhausted by sweep air was roughly correlated with evaporation rate and between 10^{-3} and 10^{-7} at boiling conditions. Fall-out reached 10^{-2}. Release data got from the evaporation of the first 30 cm^3 and the last 40 cm^3 show no clear concentration effect.

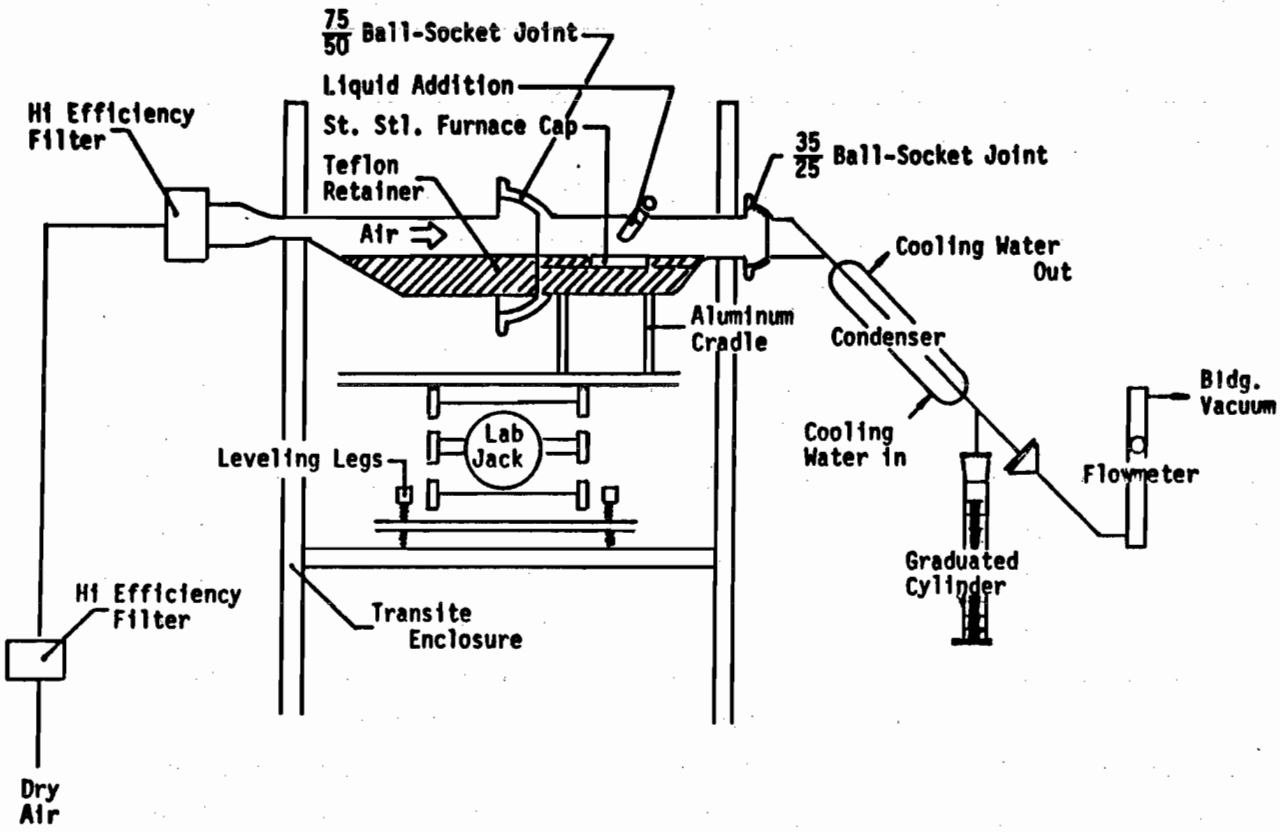

DIAGRAM OF APPARATUS USED IN AIR DRYING OF SHALLOW POOLS OF CONCENTRATED PLUTONIUM NITRATE SOLUTION

Figure 10 Experimental apparatus used by (28)

Table 11 Fractional release during air drying of concentrated plutonium nitrate solutions (28)

Run No.	Temp. (°C)	Air Velocity (cm/sec)	Sampling Time Evap. (hr)	Sampling Time Residue (hr)	Weight Percent Plutonium Found In Containment Vessel Wash	Condensate + Wash	Sweep Air During Evaporation	Sweep Air Following Evaporation
N1*	Ambient	10	24		0.0033	8.7×10^{-3}	$<10^{-7}$	--
N2*	75	10	5	20	0.00027	9.5×10^{-8}	$<10^{-6}$	$<10^{-6}$
N3	100	10	2	4	0.0046	1.7×10^{-6}	0.001	3×10^{-7}
N4	Ambient	50	24	24	0.00035	4.5×10^{-7}	2.5×10^{-7}	1×10^{-7}
N5	100	50	1-1/2	3	0.027	1.4×10^{-4}	0.003	6×10^{-7}
N6	90	50	2	4-1/2	0.00051	5.4×10^{-6}	5.3×10^{-5}	1×10^{-6}
N7	Ambient	100	24	24	0.020	7.5×10^{-8}	$<2 \times 10^{-8}$	$<2 \times 10^{-8}$
N8	50	100	2	4	0.00045	9.4×10^{-6}	1.3×10^{-5}	$<2 \times 10^{-8}$
N9	90	100	1-1/2	4	0.00013	9.4×10^{-5}	5.7×10^{-5}	3×10^{-6}

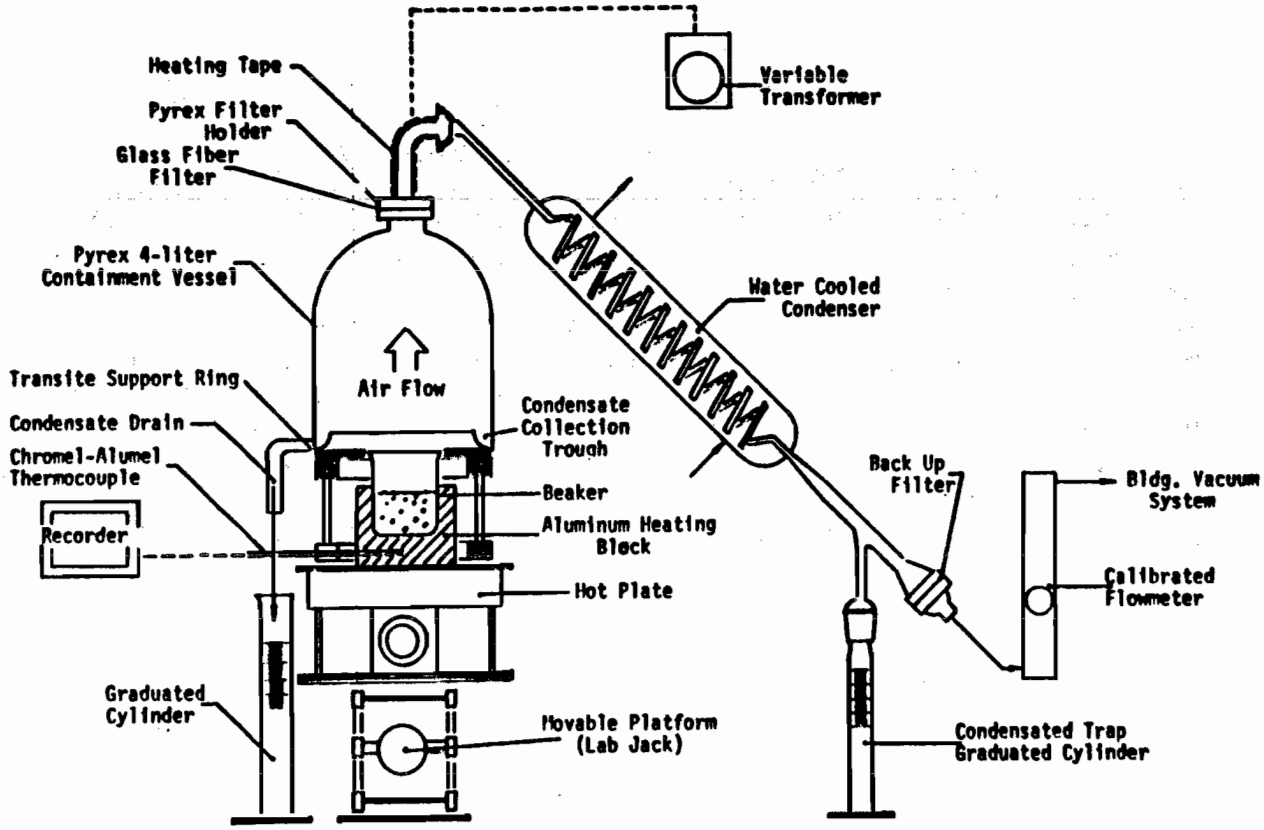

DIAGRAM OF APPARATUS USED TO DETERMINE FRACTIONAL RELEASES DURING THE HEATING OF POOLS OF PLUTONIUM NITRATE SOLUTIONS

Figure 12 Experimental arrangement used by (28)

Table 13 Fractional release during the heating of pools of plutonium nitrate solutions (28)

Run No.	Average Hot Plate Temp. (°C)	Average Boil-Off Rate (ml/min)	Period Time Heated (min)	Plutonium Recovered: Exhausted by Sweep Air (dpm)	Exhausted by Sweep Air (wt.%)	Fall-Out (dpm)	Fall-Out (Wt.%)	Visual Appearance of Solution During
A	218	1.4	63	2×10^5	.18**	2.3×10^4	.02	Boiling
B	190	0.9	80	9.4×10^4	.084	3×10^5	.27	Disturbed Surface
C	175	0.73	124	2.7×10^4	.024	1.3×10^4	.012	Disturbed Surface
D	150	0.6	151	500	4.5×10^{-4}	500	4.5×10^{-4}	Simmering
E*	220	2.1	42	∿5*	∿4.5×10^{-5}†	∿23	∿2×10^{-4}	Boiling
F	150	0.5	150	150	1.3×10^{-4}	∿3	∿3×10^{-6}	Simmering
G	164	0.66	121	6.5×10^3	.0058	1.9×10^4	.016	Distrubed Surface
H	188	1.2	64	1×10^4	.008	8×10^5	.71	Distrubed Surface
I	218	1.4	59	3×10^4	.03	2.3×10^4	.02	Boiling
J*	200	1.4	66	1.2×10^4*	.11†	1.9×10^5	1.7	Boiling

* No air flow through containment vessel, 70 µg plutonium as source. ("Airborne" is that found on containment vessel wall following this run.)

** Filter ruptured. All plutonium found in acid washes of equipment downstream of filter position.

† Plutonium in condensate.

From the CSE large scale containment tests on the behaviour of fission products (29) condensate samples were taken, evaporated to dryness, and the retention of fission products caesium and iodine determined. The experimental arrangement used by Witherspoon (30) was essentially a distillation apparatus under carrier gas flow with a Maypack sampler as backup. Less than 1.5 % of the caesium was carried over to condensate flask and filters. Since caesium is non-volatile, the observed carry-over of caesium must have been the result of mechanical entrainment.

A very similar experiment has been communicated to us by H. Albrecht, KfK, who obtained an integral carry-over of 5.5×10^{-4} from the evaporation of one litre of an aqueous solution containing all important components of a reactor coolant and a Cs-134 spiked caesium concentration of 2.5 g/liter. The carry-over decreased during the experiment.

Dexter, Evans and Jones (31) investigated the retention of iodine in irradiated solutions containing thiosulfate and other chemical additives. Potassium iodine solutions tagged with I-131 and contained in a steel can of a few dm^3 volume were irradiated for 5 hours with a water-shielded Co-60 source at a temperature of $50^{\circ}C$. The gas volume covering the solution was ventilated at a rate of 13 dm^3/min and volatilized iodine transported by this to charcoal absorber which was monitored by radiation measurement. The experimental setup is shown in Figure 14. Conditions of the experiments and volatilization results are given in Table 15. From this it can be seen that minimum volatilization was 4×10^{-4} and 6×10^{-3} under the same conditions. The authors did not check if this was due to chemical partitioning or a value established by the formation of aerosols. Some of the other experiments had shown particulate iodine which penetrated the charcoal.

Manowitz et al. (32) developed a system for the decontamination of radioactive waste solutions containing non-volatile fission products. The system consisted of an evaporation unit and a de-entrainment device. Various technical modifications were chosen and the decontamination effect measured with and without de-entrainment device. Results are presented as decontamination factors defined as the ratio of the specific activity of the evaporation residue and the distillate. In Figure 16 curves

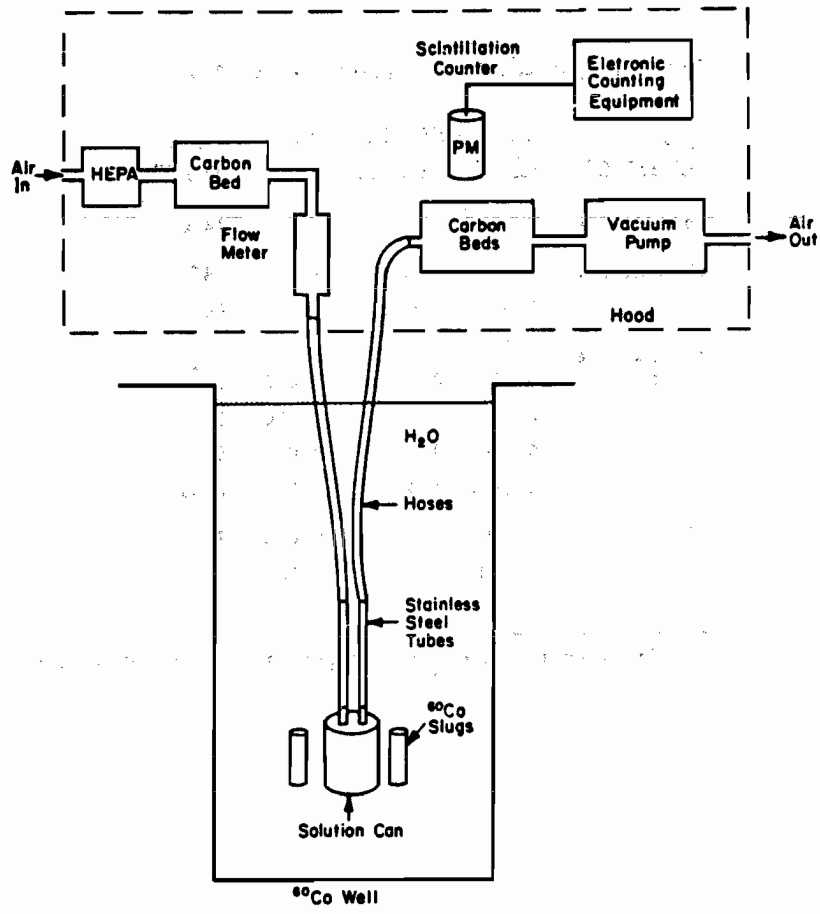

Figure 14 The iodine evaporation experiment (31)

Table 15 The iodine evaporation experiments - experimental conditions and results

Iodine Evaporated After Exposure to 10^8 Rad

Type Experiment	*Concentrations, wt%*			*Iodine Evaporated, %*
	CsI	*$Na_2S_2O_3$*	*KOH*	
No Additive	0.010	-	-	14.6
Thiosulfate	0.010	0.014	-	94[a]
	0.010	0.014	-	96[a]
Thiosulfate and KOH	0.010	0.014	0.006	30[a]
	0.010	0.1	0.006	96
	0.010	1.0	0.006	0.044
	0.010	1.0	0.006	0.55
KOH	0.010	-	0.006	2.5
	0.010	-	0.050	1.2

a. Experiments that gave the penetrating iodine species.

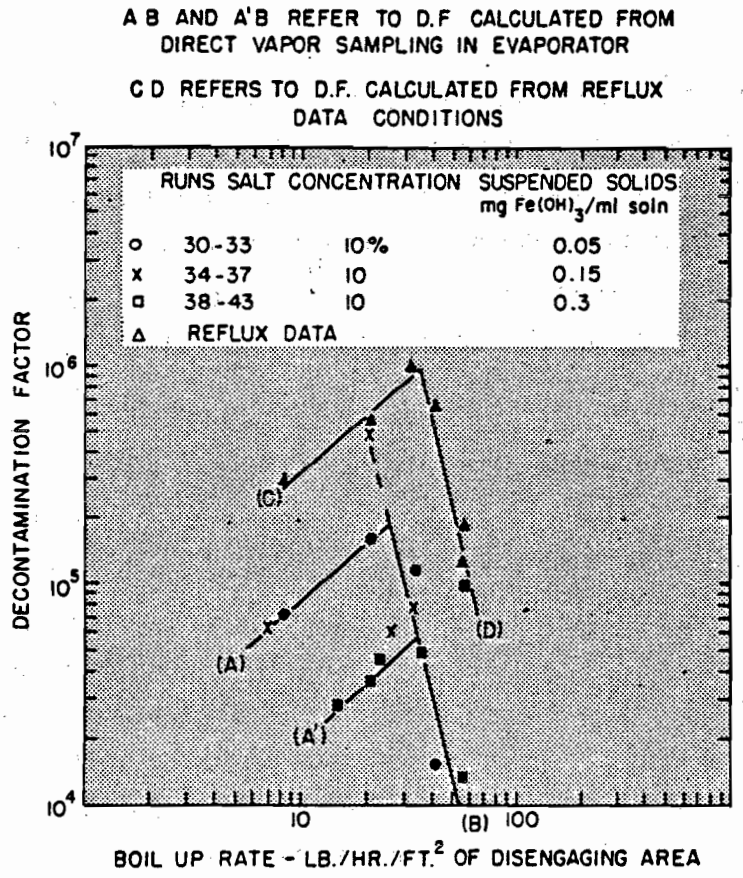

Effect of boil-up rate on the decontamination factor for liquid entrainment-submerged coil evaporator.

Figure 16 Results of decontamination experiments (32)

AB and A' B represent results obtained without de-entrainment device. From this it can be seen that decontamination was between 10^{-4} and 10^{-5} depending on boil-up rate and content of suspended solids from rusting. Better decontamination was obtained at lower solids content. Further, the authors suggest different behaviour of droplets and particles with respect to carry-over by stating that "it was possible to distinguish between entrained solids carry-over and liquid entrainment" by different radionuclide composition.

Garner et al. (33) investigated the main parameters of liquid entrainment in evaporators. They used an evaporator pilot plant operating under reduced pressure of 250 mm Hg and equilibrium conditions. Sugar solutions were chosen for the test since they show little influence of sugar concentration on density and surface tension of the solutions. Thus the concentration chiefly affects the viscosity. The sugar content of the evaporator sump and the condensate are measured by means of the refractive index and a colorimetric method. From this the liquid content in the vapour is calculated in ppm (apparently assuming that the sugar concentration in the sump is the same as in the droplets). The results of a series of measurements with systematically varied parameters are shown in Figure 18. From these an increase in entrainment with increasing vapour generation rate and concentration can be recognized. Variations in liquid level (which implies variation in vapour space height) were of low significance. From the maximum entrainment of 800 ppm reported a retention factor of about 10^3 can be estimated, defined as the concentration ratio of the sump and condensate.

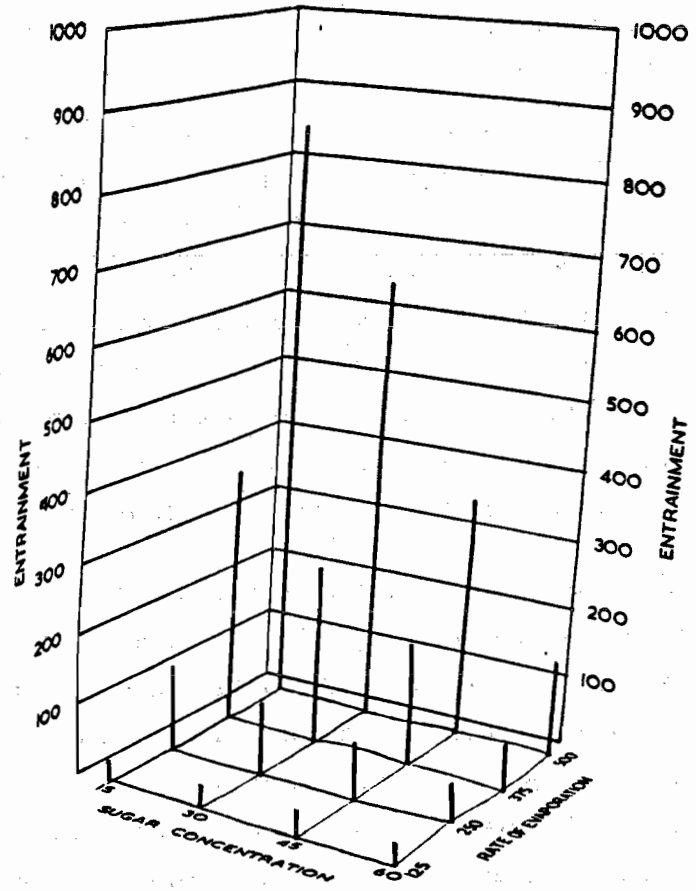

Figure 17 Results of entrainment experiments at very high solute concentration (33)

In 1954 Garner et al. (34) reported a determination of the size distribution of entrained droplets and the total entrainment. Under various operating conditions experiments were made using a pilot plant vertical tube evaporator (12" diameter) and a small single vertical heating tube glass evaporator (4" diameter). Water and solutions of potassium nitrate were evaporated and liquid samples taken from the condenser and the vapour line condensates. Nitrate determination was carried out by gravimetry and a colorimetric method. Droplet samples were drawn in the vapour space at different distances from the liquid surface by a two-stage impactor device. Droplets collected on this were sized and counted under a microscope. The collection of droplets below 8 µm was not complete but was corrected for. From condensate nitrate analysis and droplet measurements entrainment of liquid in the vapour was calculated.

The authors found that more than 95 % of the droplets collected were below 20 µm. In spite of the large numbers of these droplets, the total amount of entrainment was essentially due to droplets above 100 µm. This is shown by Figure 18. The vapour line had an appreciable retention effect on the entrainment of large droplets. Liquid level in the evaporator was of minor influence. Increased vapour velocity was found to be correlated to increased entrainment (Figure 19). Table 20 shows a comparison of entrainment determined by chemical analysis of the condensate and by droplet analysis. From this total entrainment is seen to lie between 10^{-5} and 10^{-3}.

Results from the glass tube evaporator showed entrainment of the order of 10^{-4} and reduction of entrained amount by foaming at the same rate of evaporation.

Shor, Ward et al. (35) determined radioactive carry-over in boiler units. Measurements were done on a 3" diameter laboratory scale evaporator, a pressurized boiling loop of industrial scale (5" diameter) and a small BWR. The boiler water of the laboratory scale evaporator was spiked with caesium-137-chloride. Condensate was continually counted and

from the ratio of its concentration to that of the boiler water decontamination factors (DF) were determined. Initial DF was lower than equilibrium DF reached after several hours. This time behaviour was explained by accumulation of dissolved solids in the boiler during the experiments. Equilibrium DFs were of the order of 10^5. In the boiling loop pressure was varied between 150 and 160 psia and sampling was done at three different levels above the water surface at the same time. DFs were determined between 1.1×10^4 and 6.8×10^4. Also at this installation relatively high initial release and low DF was found. Values found after 100 or 200 minutes were regarded as near to equilibrium and reported as results. Entrainment was correlated to the boiling rate. Pressure, sampling position and sampling mode were of minor importance. Liquid and vapour sampling at the BWR was done at four different positions and from "involatile" Na-24 activity decontamination factors between 6×10^3 and 1.5×10^4 were calculated, depending in the known manner on vapour velocity. Results from the three systems are presented together in Fig. 21, which confirms the paramount influence of steam velocity. Differences between the systems are explained by the different amount of wall effect in droplet reduction.

Experimental values for the entrainment measured by Sterman et al. are reproduced from the original report in the 1960 review of entrainment given by Yeh and Zuber (36). From these results in Figure 22 entrainment values are seen between 10^{-2} and 10^{-5} depending on the pressure and a dimensionless group which essentially means the vapour flow conditions. High pressure and vapour flow enhance entrainment. The method of measurement is not known. The dimensionless group $\mu_o''^2/\alpha g H_v$ is a combination of the vapour velocity u_o'', the volume fraction α of vapour in the water, the gravitational constant g, and the vapour space height H_v. It is seen that influence of the vapour flow conditions implies not only influence of the energy input to the system but also influence of the vapour space geometry if the evaporation device is changed.

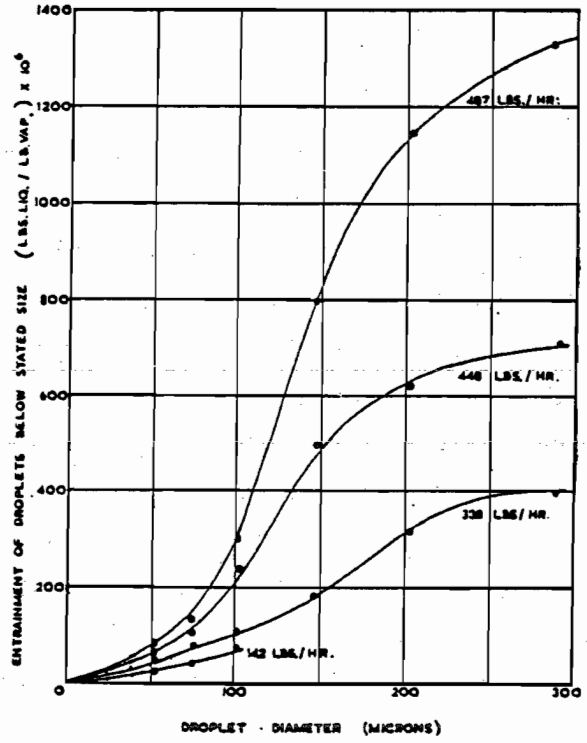

Figure 18 Size-dependent entrainment of droplets obtained at varied gas velocity (34)

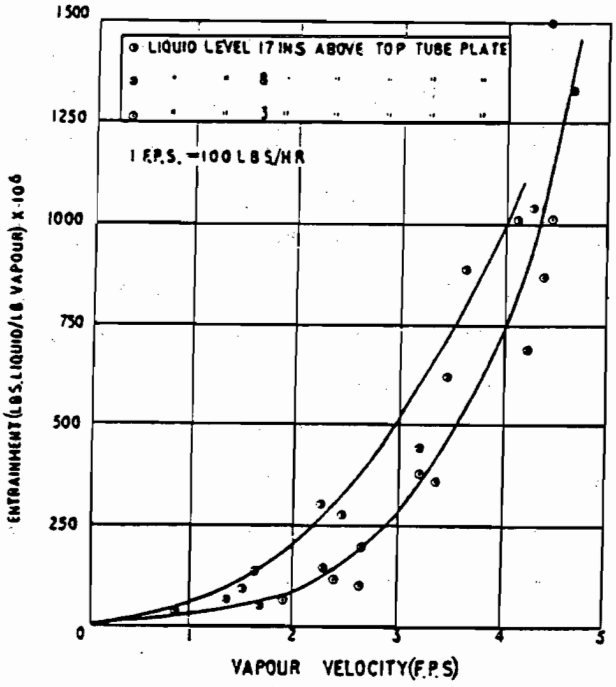

Figure 19 Entrainment vs. vapour velocity, obtained at varied height above the liquid (34)

Table 20 Entrainment results obtained by different methods (34)

Rate of evapn. (lb./hr.)	Entrainment by chemical analysis (lb. liq./lb. vap.) × 10^6	Total entrainment of droplets (lb. liq./lb. vap.) × 10^6	Entrainment of droplets below the terminal velocity droplet (lb. liq./lb. vap.) × 10^6
94	35	38	38
182	44	44	42
200	48	66	50
252	45	128	117
279	59	105	99
283	120	206	146
338	132	396	241
355	99	360	312
463	354	868	418

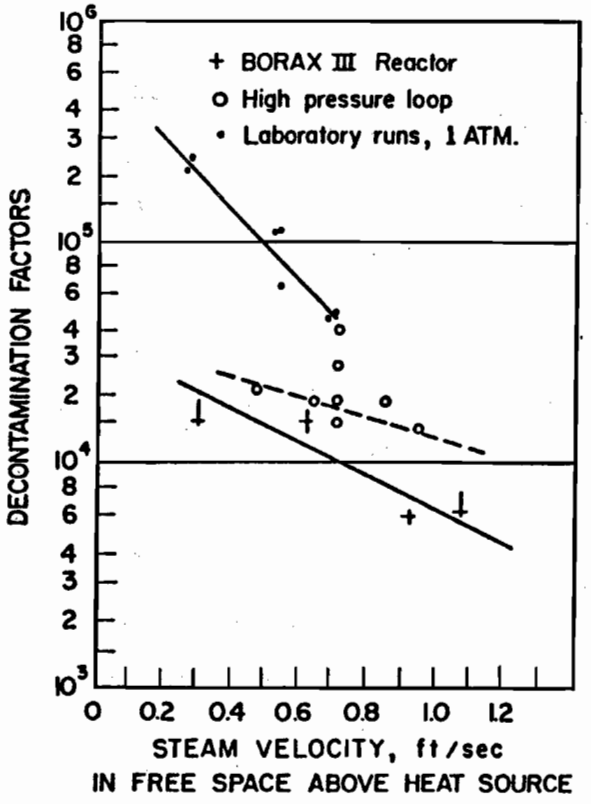

Figure 21 Decontamination factors obtained by evaporation of aqueous solutions in three different installations (35)

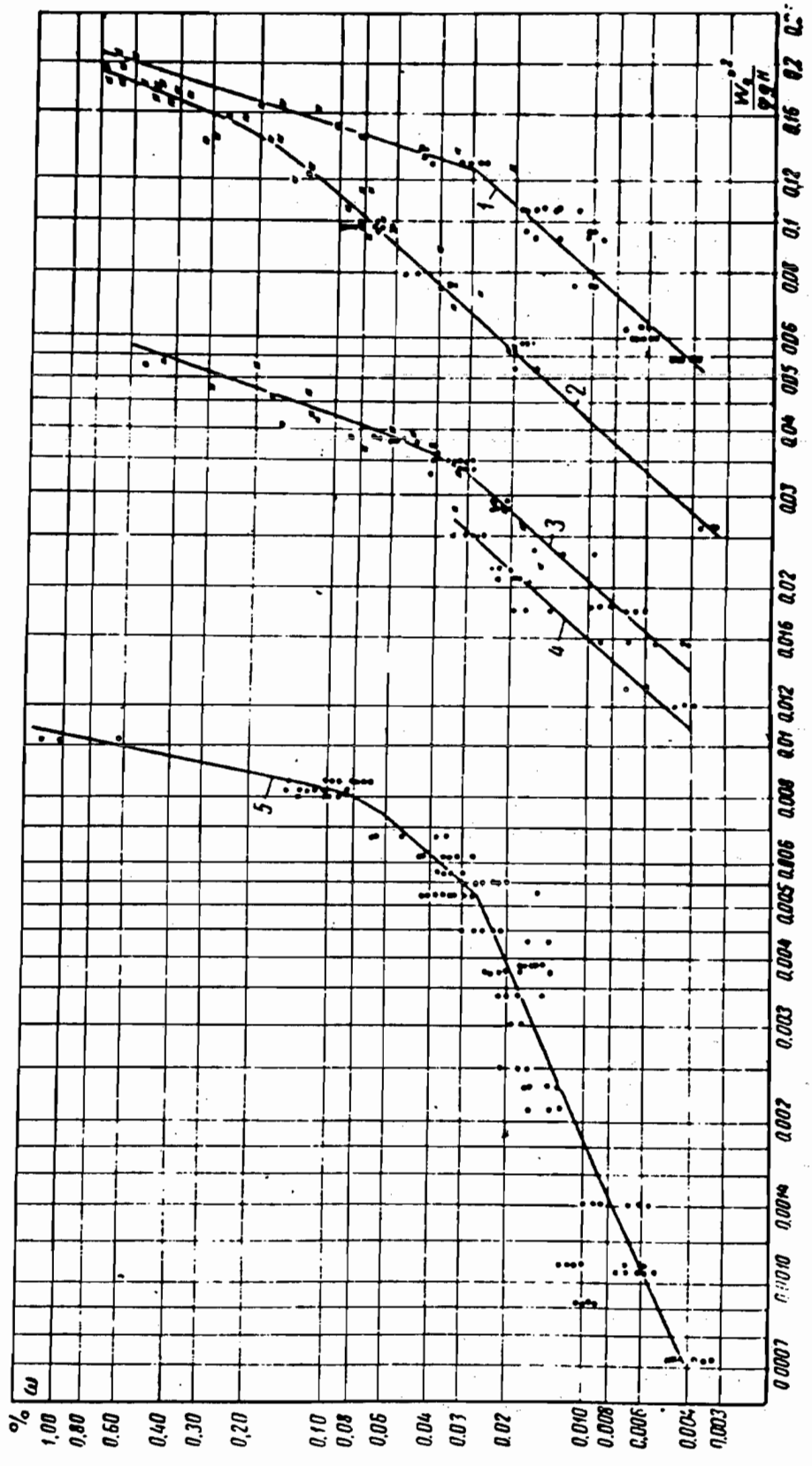

The Entrainment E(%) as Function of Pressure and of the Dimensionless Group $N = \frac{\mu_o''^2}{\alpha g H v}$.
(Ref. 41)

1:P = 17 atm; 2:P = 36 atm; 3:P = 91 atm; 4:P = 110 atm; 5:P = 185 atm.

Figure 22 Entrainment at varied pressure (reproduced from (36))

Heger, Wäscher et al. (37,38) conducted bubbling experiments in simulated reprocessing plant components in order to get information about the generation of aerosols in the reprocessing of nuclear fuels. First measurements were done on a 50 dm^3 air-stir container filled to different levels with solutions of sodium nitrate of varied concentration and content of further additives. The stirring air flow velocity was of the order of 10 m/h and also varied. The container gas phase was analyzed by an optical method for aerosol number concentration and size distribution of the generated aerosol. The mass concentration of aerosols was determined by weighing and sodium analysis of filter samples. The sodium nitrate concentration in the air above solution of 10 % nitrate and 10 % nitric acid was 50 - 10^3 $\mu g/m^3$ and was strongly enhanced by adding 200 ppm TBP because of reduced surface tension (Figure 23). TBP was enriched in the aerosol compared to the bubbled solution. The size of the generated aerosols was bimodally distributed between 0.1 and 6 µm with maxima at 0.3 and 0.8 µm approximately. TBP addition increased the generation of the larger-size fraction. Increased nitrate concentration from 10 % to 30 % effected a 5 to 10-fold increase in aerosol generation. The same analytical methods were applied to an air-lift and similar results were obtained.

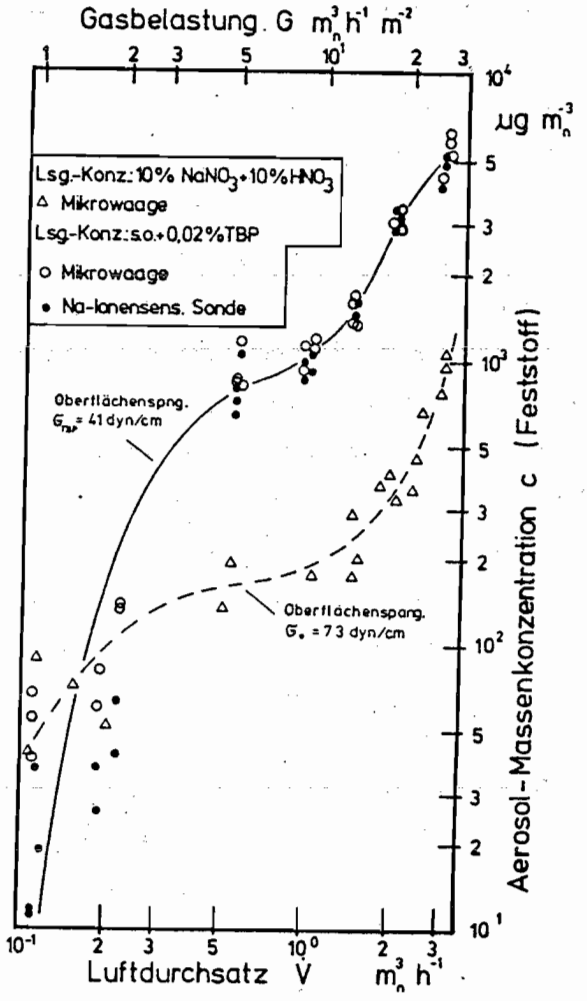

Figure 23 Concentration of airborne solids vs. gas flow or gas velocity (upper scale) measured at varied surface tension (37)

In the preceding chapter laboratory scale experiments and industrial-scale evaporator measurement are both shown to result in entrainment values in the range from 10^{-2} to 10^{-7} irrespective of scale and material flow pattern. Continuous experiments result in entrainment values relative to the evaporation of the solvent and related to only one set of experimental conditions while discontinuous experiments give the integral released fraction of the solute up to the state of evaporation reached in the experiment.

From the evaporator measurements it is seen that the geometry of the vapour space and the gas velocity are important parameters. At low gas flow and at great distance from the liquid surface low entrainment was measured and vice versa. High pressure - which is not relevant for a post-rupture reactor containment - results in enhanced entrainment. Increased surface tension is correlated with decreased entrainment. Influences of some importance have been observed with respect to concentration, viscosity, solids content and foaming.

Determination of entrainment has in many cases been carried out from the measurement of entrained solids. Since these are the object of interest in the present study this may be considered as favourable. But the entrainment of different solids may be different and also different from entrainment determined by measurement of entrained liquid. Comparison of the entrainment values obtained by two different methods in the same system (34) showed a difference up to a factor of 2. Chemical analysis yielded the lower values. In chapter 3 it is shown that chemical enrichment and depletion in entrained aerosols is an often-observed fact and may amount up to half an order of magnitude.

Based on the apparent geometric differences between a vigorous boiling evaporator and a reactor building which should lead to lower entrainment in the latter case, the preliminary conclusion is that droplet generation from the sump may be of importance similar to particle resuspension.

3. Mechanisms and parameters of resuspension and re-entrainment

In this chapter information has been gathered from the literature which may be useful in the identification of possible mechanisms of particle resuspension and aerosol generation and the important parameters related to them. From the preceding integral measurements we have seen that the conditions of gas flow are main parameters. But detailed discussion of the mechanisms will show that the properties of the medium from which the droplets and particles are released are important, too.

Bubble bursting at the gas-liquid interface is the most important mechanism in the generation of entrainment by liquid droplets. From (16) we can suppose that it is also important in the revolatilization of suspended particles. For this reason literature information on the processes and parameters involved in bubble-induced droplet generation is compiled in this chapter.

As is shown below, bubble size is a very important factor for the number and size of droplets generated by bubble bursting, and it is therefore useful to know the bubble size under boiling conditions. The fundamental relation for bubble size in a liquid is the equilibrium between surface tension and internal overpressure. The internal pressure results from the vapour pressure on the liquid. Once the bubble is generated, it rises through the liquid and grows due to decreasing hydrostatic pressure. These fundamental relations are known. The size of steam bubbles generated in ordinary boiler water at a horizontal steel surface has been measured to range from 0.5 to 5 mm at low pressure and nucleate boiling (39). Some uncertainty is brought into this clear situation by further effects: because of the reduced vapour pressure of concave surfaces a bubble nucleus is required for the generation of small initial bubbles. This may be a rough surface or a suspended particle. The formation of the macroscopic bubble and its detachment from the surface is influenced by the contact angle of the system and the degree of superheating. The free bubbles may coalesce or divide during their ascent to the surface. This

effect will be more important at high bubble flow. Thus, clear predictions are not easy for realistic boiling situations. In general, a broad bubble size distribution is expected instead of a well-defined single diameter.

When the bubble has reached the surface it will take a form between sperical and hemisperical - depending on its size. During this phase the liquid in the bubble's film dome runs down and the film thins until the internal pressure of the bubble (which is higher in small bubbles) breaks it. The breaking of the film is the subject of discussion but it is certain that small droplets are formed as the film breaks (34, 40-42). After the pressure in the bubble is released the liquid crater which is left collapses and an ascending jet of liquid is formed which decays to droplets after reaching a critical length (43): see fig. 24.

For both mechanisms of droplet formation there is a limiting bubble diameter. Jet drops are formed only from bubbles smaller than 5 or 6 mm. Film droplets are from bubbles larger than approximately 0.2 mm. These limits establish three regions of droplet formation: in the region below 0.2 mm bubble diameter only jet drops will be formed. This region is of little interest for the purposes of this study, because it is connected with high pressures (44).

The region with the possibility of both mechanisms, between 0.2 and 6 mm, has been best investigated. The number of film drops produced by bubble bursting is correlated to the film area and will reach several hundreds at the upper diameter limit of this region. Determination of film droplet diameters is difficult but experimental values are given by (34,40,41). As can be seen in figs. 25 and 26, the size/number distribution will be between 1 and 50 µm with most droplets below 25 µm. The mean diameter increases with decreasing bubble size. In terms of released volume or mass this counters the decreasing number of droplets.

A mass distribution of entrained droplets over a range of droplet sizes was obtained by conversion of data which were measured by Garner (34) on the small glass-tube evaporator (fig. 27).

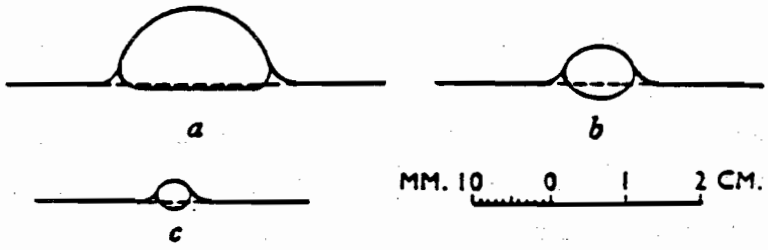

fig. 24 a) shape of floating bubbles (35)

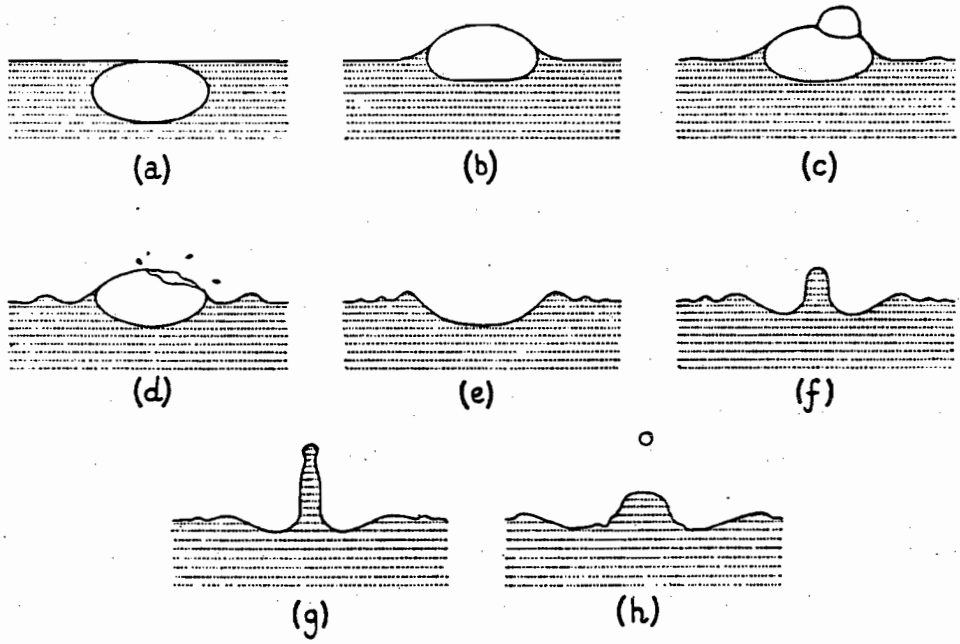

fig. 24b) mechanism of bubble breaking and droplet generation (37)

Figure 24 Shape of floating bubbles and mechanism of droplet generation by bubble breaking

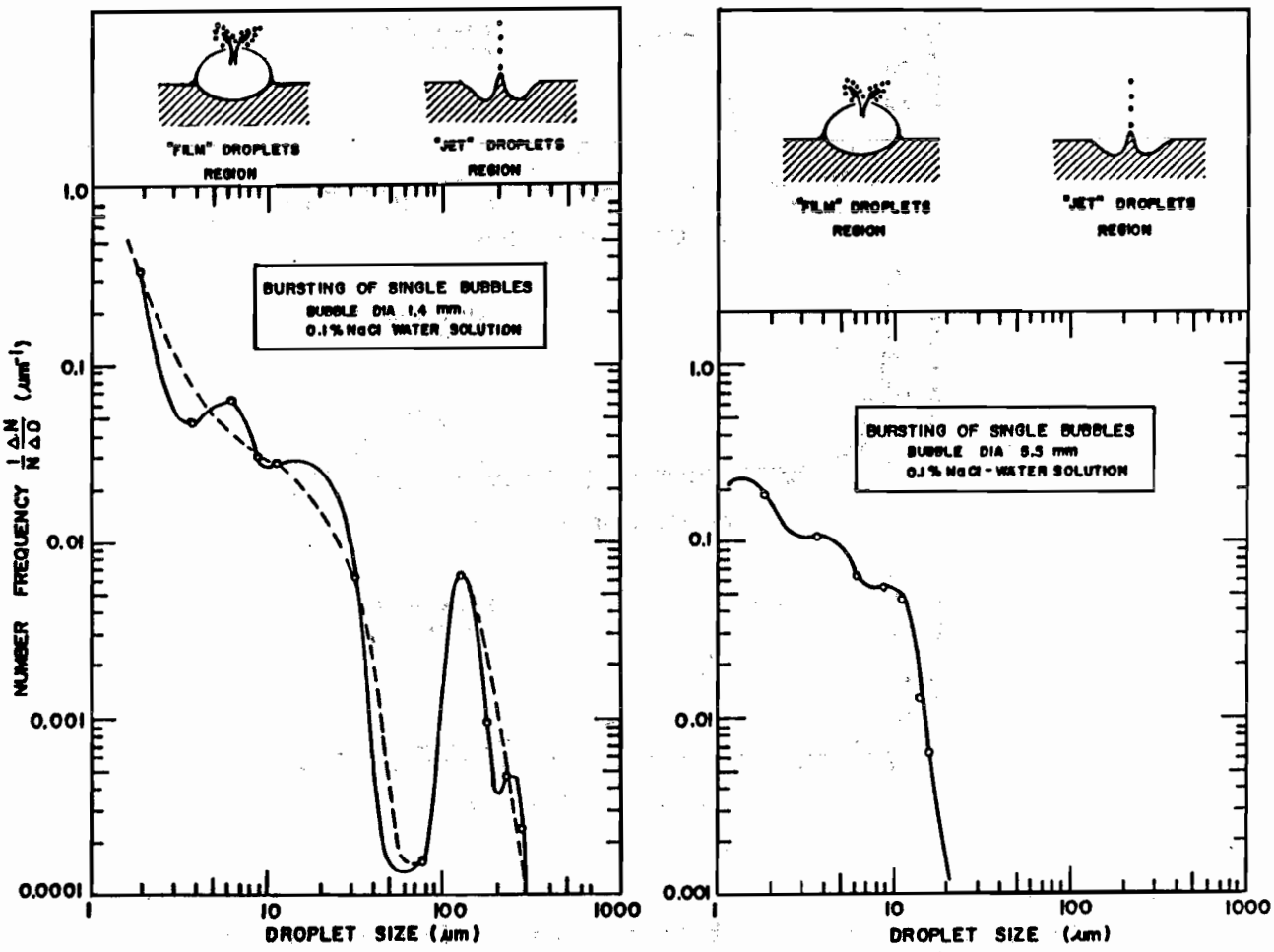

Figure 25 Size distribution of bubble induced droplets
(frequency distribution) (41)

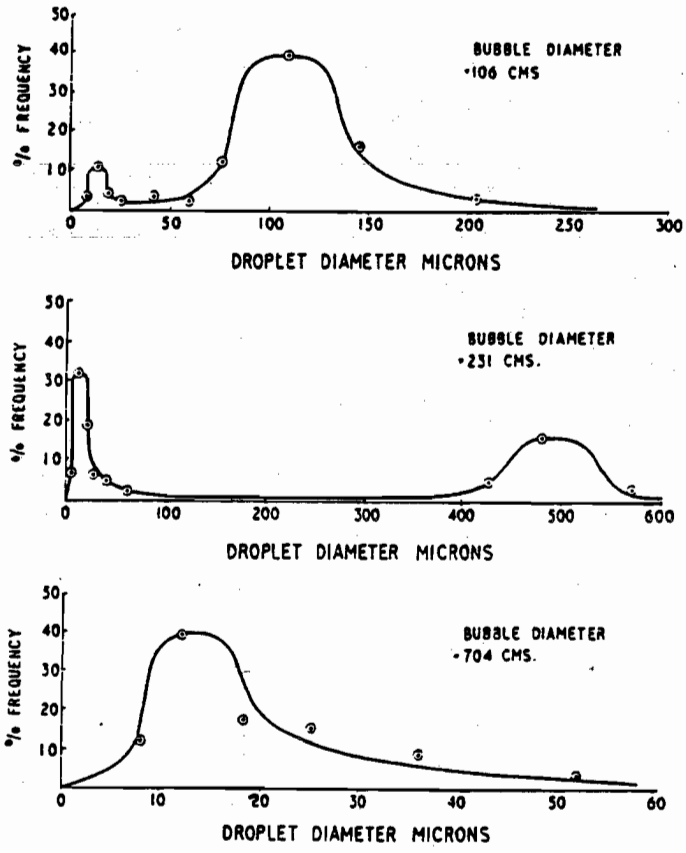

Figure 26 Size distribution of bubble induced droplets (frequency distribution) (34)

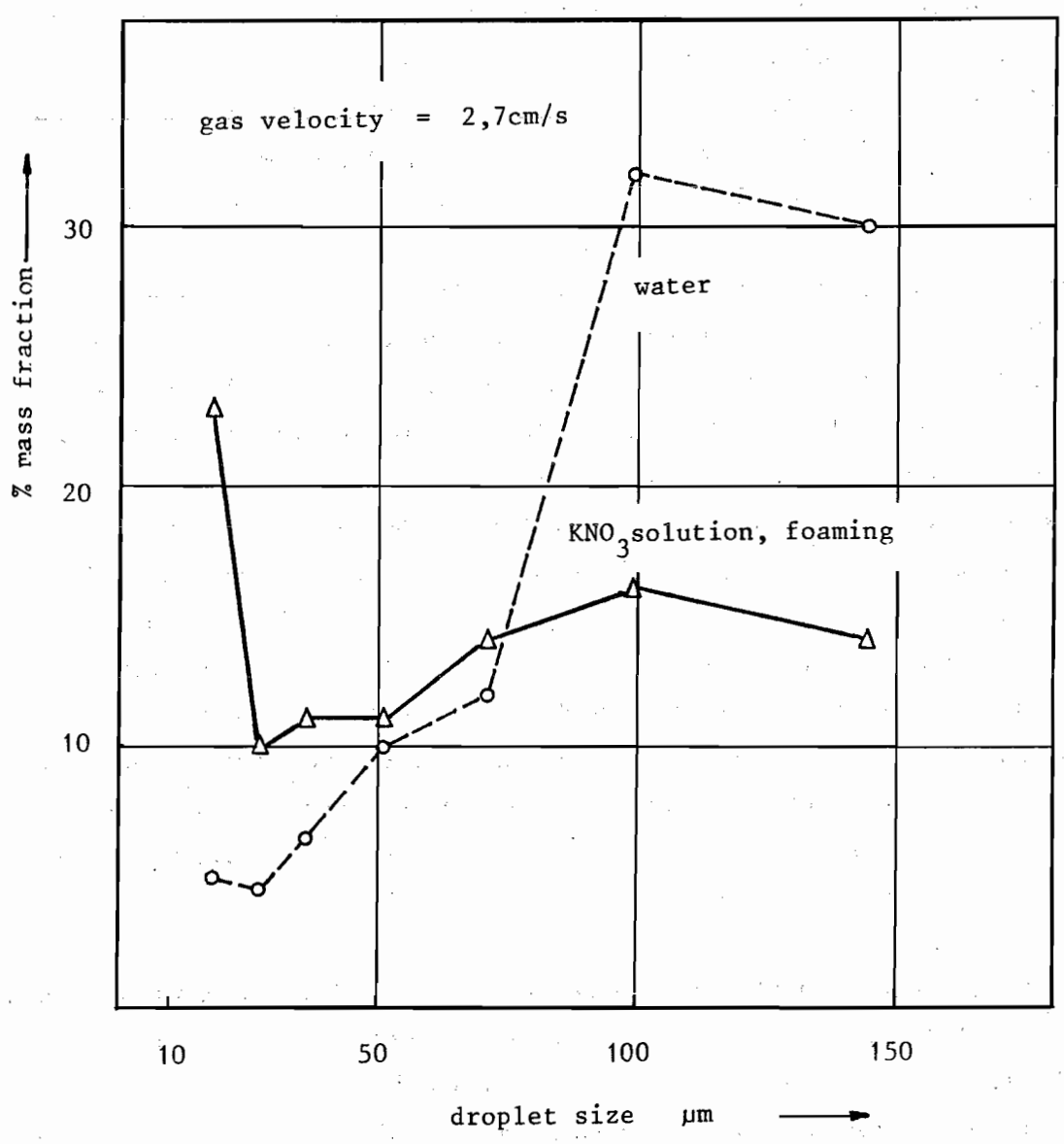

Figure 27 Size distribution of entrained droplets (mass distribution) (34)

Most of these results have been determined by cold bubbling of water and solutions. Increased temperature will produce smaller droplets. Surface tension in the system air/water and steam/water is very similar.

From the same bubbles a number of jet droplets will be formed which depends on the bubble size. Larger bubbles form only one droplet. Beginning from approx. 2 mm bubble size, a second droplet is ejected and from very little bubbles up to six droplets may be generated. With increasing viscosity and surface tension this number seems to decrease and increase respectively, but little information is given in the literature. The diameter of the jet droplets is correlated to the bubble diameter. From the available experimental results compiled in fig. 28, it can be roughly estimated that the droplet diameter will be 20 % of the bubble diameter, i. e. 100 to 1000 µm. Experimental size distributions have already been shown in figs. 25 to 27. It is suggested that droplet size is independent of surface tension (45) and negatively correlated to viscosity, but the effects have not yet been quantified. The jet drops rise to a height of up to 20 cm from the liquid surface and fall back to it, possibly inducing secondary drops. The ejection height has been shown by experiment to be reduced by enhanced viscosity. For ejection height see fig. 29. The processes have been reviewed by (36,43). Jet-droplet measurements have been reported by (34,40,41,45-49). Experimental results are from cold bubbling of aqueous systems. The influence of temperature has not been investigated.

In the third region of bubble sizes above 6 mm, droplet formation is due only to film droplets. Experimental measurements for undisturbed "big" bubbles (say 20 or 40 mm) are, to our knowledge, not reported in the literature. Foaming evaporators are considered to show entrainment only due to film droplet formation, because jet drops are caught by the foam. This results in general in a strong reduction of entrainment unless the foam itself is entrained to the vapour line (34).

The presence of chemicals influences the formation of aerosols from liquids. On the other hand, aerosol formation processes lead to chemical effects on the particles and droplets formed. Influence of electrolytes on the entrainment has been observed (44). According to these measurements, the maximum entrainment with respect to varied gas velocity depends to a varying degree on the concentration and nature of dissolved salts.

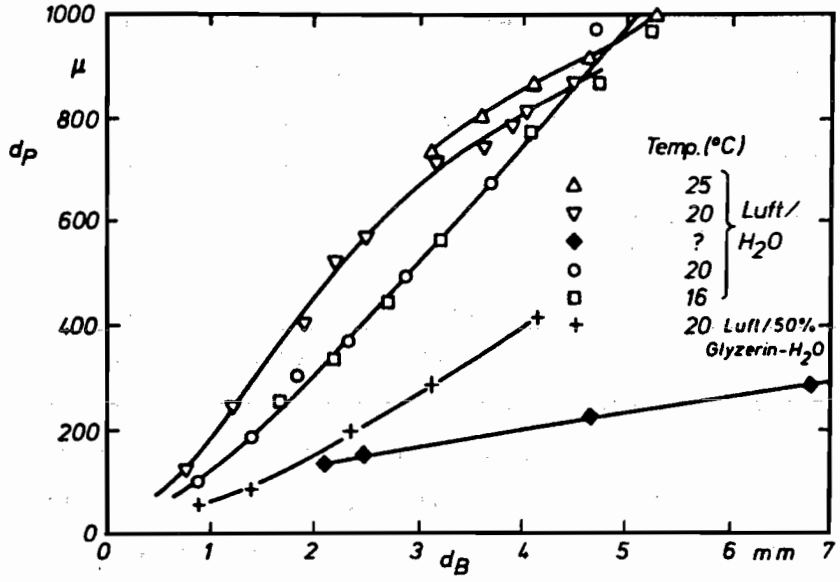

Figure 28 Jet droplet diameter vs. bubble diameter (several authors, compilation by (43))

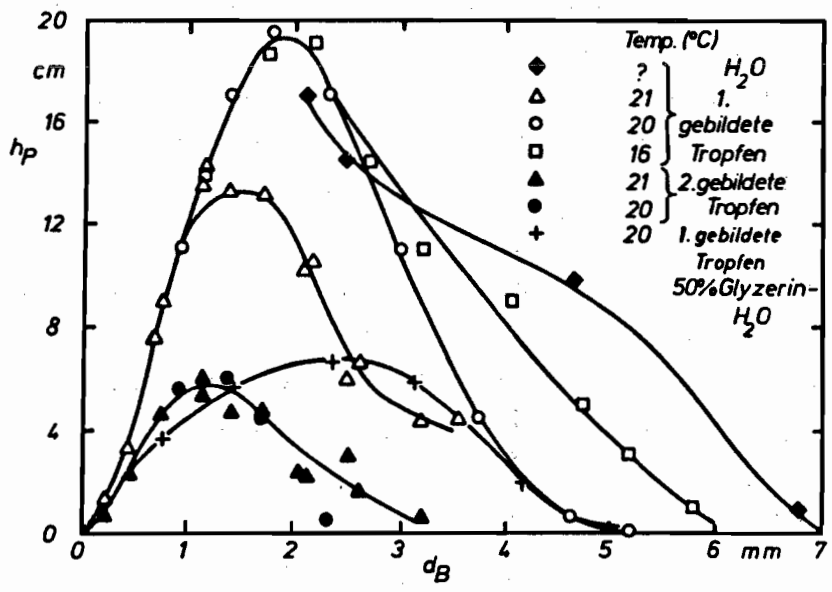

Figure 29 Ejection height of jet droplets vs. bubble diameter (several authors, compiled by (43))

The variation was within a range of 5. Similar observations were made by (48) in investigation of aerosol generation from dilute sodium chloride solutions in a bubbler. The effect of varied NaCl concentration between 10^{-4} and 10^{-1} M was an enhancement of the aerosol densities obtained by roughly an order of magnitude.

Baumgärtner et al. (50) investigated the release of fission products from simulated high activitve waste solutions (HAW) under evaporation. Aerosol formation during evaporation was studied by bubbling of salt and HAW solutions. Released aerosols were dried and collected by membrane filters or an aerosol sizing centripeter. Despite the somewhat preliminary nature of the experiment some interesting qualitative results were obtained. Separated and mixed solutions of europium nitrate, strontium nitrate, and caesium nitrate, sodium chloride and potassium permanganate were bubbled and the known influence of bubble size, surface tension and viscosity on the aerosol release were found. Entrained liquid volume fraction in the flowing gas was of the order of 10^{-8}. No flow data were reported. Temperature was ambient. Aerosols were bimodally size-distributed with maxima between 0.1 and 1 µm. Formation of manganese oxide particles from permanganate content in mixed solution with europium nitrate was of strong influence on the size distribution of the europium and manganese aerosol generated by air bubbling. Influence on total released amount is not reported.

Simulated HAW solution - containing several elements in nitric acid solution - released significantly more aerosols than expected from bubbling of salt solutions and correcting for concentration differences. Analysis of the chemical composition of the aerosols showed marked effects: Sodium was depleted in the aerosol compared to the solution by a factor of 5; aluminium, iron and zirconium were enriched by a factor of 2 - 4. This is explained by different behaviour of hydrolyzing and non-hydrolyzing ions with respect to surface concentration changes.

Similar chemical fractionating is known from the salt aerosols generated in the sea (51-53) by bursting of bubbles. This is understood by looking at the flow patterns in bursting bubbles. From (54-55) we see that jet droplets are produced exclusively from the layer ($\lesssim 1$ µm)

irrediately surrounding the bubble, thus giving droplets of a chemical composition representative of the liquid surface but not of the bulk liquid. Similar effects may be possible at the release of film droplets.

This mechanism is extended to the release of particles by the work of (16,56-58). Measurements of bacteria release to the air from an aqueous environment by bubbling were made and considerable enrichment of one particular variety of these was found in the released mass. Some doubt on this is discussed in (16). The bacteria were approx. 1 µm in size. The authors believe that they were collected during bubble rise and that the presence of surface-active contaminants may be of influence.

Dissolved inorganic salts, glycerin and suspended particles were found to stabilize bubbles at the liquid surface (34). This may result in foaming, with subsequent reduction of droplet ejection. On the other hand bubbling removes small particles from the surface and effects transport to the gas phase. This is known from experience with calcium carbonate - accumulated in boilers. The suspended solid particles are transported to the surface by adherence to the rising steam bubbles, providing the particles are not wettable by the liquid. A discussion of the critical particle diameter for this mechanism is given by (39).

From the information available in the literature it is seen that the number and the size of bubble-induced droplets depend on the viscosity, surface tension, and density of the liquid. These in turn are dependent on the basic properties temperature, pressure and chemical composition. Bubble size is one of the most important factors. It is influenced by the above-mentioned parameters, but additionally dependent on the properties of the surface at which the bubbles are generated, on the boiling conditions and on random processes of bubble-bubble interaction during the rise through the boiling liquid. Thus for practical purposes it may be regarded as an independent parameter influencing droplet generation.

In spite of a lot of work done in this field, a quantitative prediction of entrainment from known properties of the system is not yet possible. Some qualitative features which may be of great importance can be easily seen:

- the influence of surface effects on the amount and composition of the generated aerosols,
- the possibility of chemical enrichment and depletion of substances in the aerosols,
- the existence of two groups of droplets with different mean size and amount of airborne mass,
- the limited range of the ejected jet droplets due to their initial velocity.

The latter two facts should be of influence on the transport of the generated aerosols.

With regard to suspended solids the experimental base is even poorer. The qualitative facts known are that they may enhance the stability of bubbles at the surface, thus leading to lower entrainment or even foaming, and that they are volatilized by bubbling. The condition for this is that their mass should not be too great for them to be carried at the liquid surface by buouyancy and the surface forces.

4. Modelling of droplet entrainment

The state of theory has been reviewed in 1960 by Yeh and Zuber (36) and in 1983 by Kataoka and Ishii (59). In 1960 the theory was in general restricted to evaporator application but the more complete mathematical assessment of the entrainment performed by (59) promises applicability for the present purpose as well.

The entrainment of liquid in a vapour generated from a liquid pool is dependent on the conditions of boiling and gas flow. At least two different boiling regimes have to be distinguished. At lower evaporation rates, when the fraction of bubbles in the liquid is below 30 %, discrete steambubbles rise through the liquid and burst at the surface. The droplets are generated by the mechanism which has been outlined in chapter 3. At higher evaporation rates, the liquid becomes turbulently mixed and progressively disintegrated at the surface. The surface disintegration by the rising steam is responsible for the generation of droplets. At very high gas flow, which may be considered as a third (unfavourable) boiling regime, modelling for the intermediate region does not provide an adequate description. In this boiling regime extensive splashing and foaming occurs.

If, on the other hand, the boiling conditions and the geometry of the evaporation device are kept constant, marked changes of the amount of entrainment will be observed at different heights above the boiling surface. The entrainment to the gas layer in the vicinity of the surface is governed by the splashing of the moving liquid and shows no important changes dependent on height. The entrainment in the adjacent layer is dominated by droplets whose settling velocity is greater than the gas velocity but which are airborne due to the momentum from the mechanism of generation. In this layer, the amount entrainment decreases with increasing distance from the liquid-gas interface. Only droplets whose settling velocity is smaller than the gas velocity are transported to the top layer by the gas flow. In this region, the decrease in the amount of entrainment is due only to the wall effect of the evaporation device and may be strong or negligible, depending on the geometric conditions of the vapour space.

The different operating conditions of evaporators are shown in Fig. 30. In general, evaporators are operated in the second boiling regime (Fig. 30c), where surface disintegration is the most important mechanism of droplet generation and where the vapour space height is inside the region of the momentum controlled entrainment. For the purpose of the present study the boiling regime of discrete bubble flow and heights which are outside the range of the large droplets are more important, as will be shown later.

The entrainment can be calculated in the distinct regimes by using equations of the type.

$$\text{entrainment} = \text{constant} \cdot \text{vapour velocity}^{n}.$$

In the regime of discrete bubble flow the exponent is unity, and it changes to three in the second regime. At very high gas flow, a value of up to twenty may be reached. The constant is composed of the dimensions of the evaporation device, material properties of the system (which are chiefly dependent on the temperature) and empirically determined numbers which fit the measured entrainment.

The transition from the low gas flow regime to the intermediate flow regime occurs at a gas flow greater than approximately 15 cm/sec. For the entrainment due to discrete bubble flow a formula of this type is given by (59):

$$E = N^{1.5} \cdot D^{*1.25} \cdot d^{-0.31} \cdot v^{*} \cdot h^{*-1}$$

where v^{*} is a dimensionless expression for the vapour velocity which is proportional to the real vapour velocity, N is a dimensionless expression which includes the material properties of the gas/liquid system as surface tension and viscosity, d is a dimensionless correction term for the density conditions, and h^{*} and D^{*} are dimensionless expressions for the height above the pool and the hydraulic diameter of the vessel. For the entrainment in the wall deposition controlled region only one formula is given for the entrainment without any difference

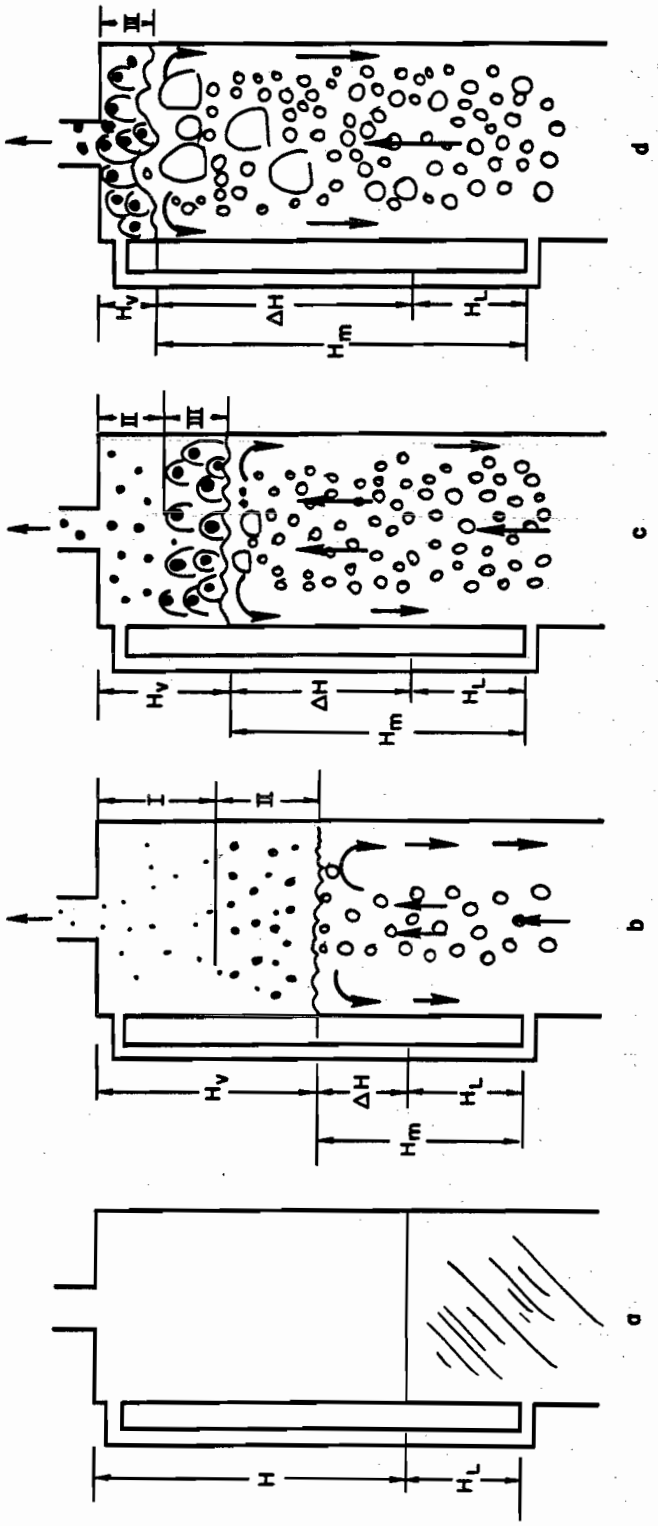

Figure 30 Schematic of evaporators working under different conditions of entrainment (36)

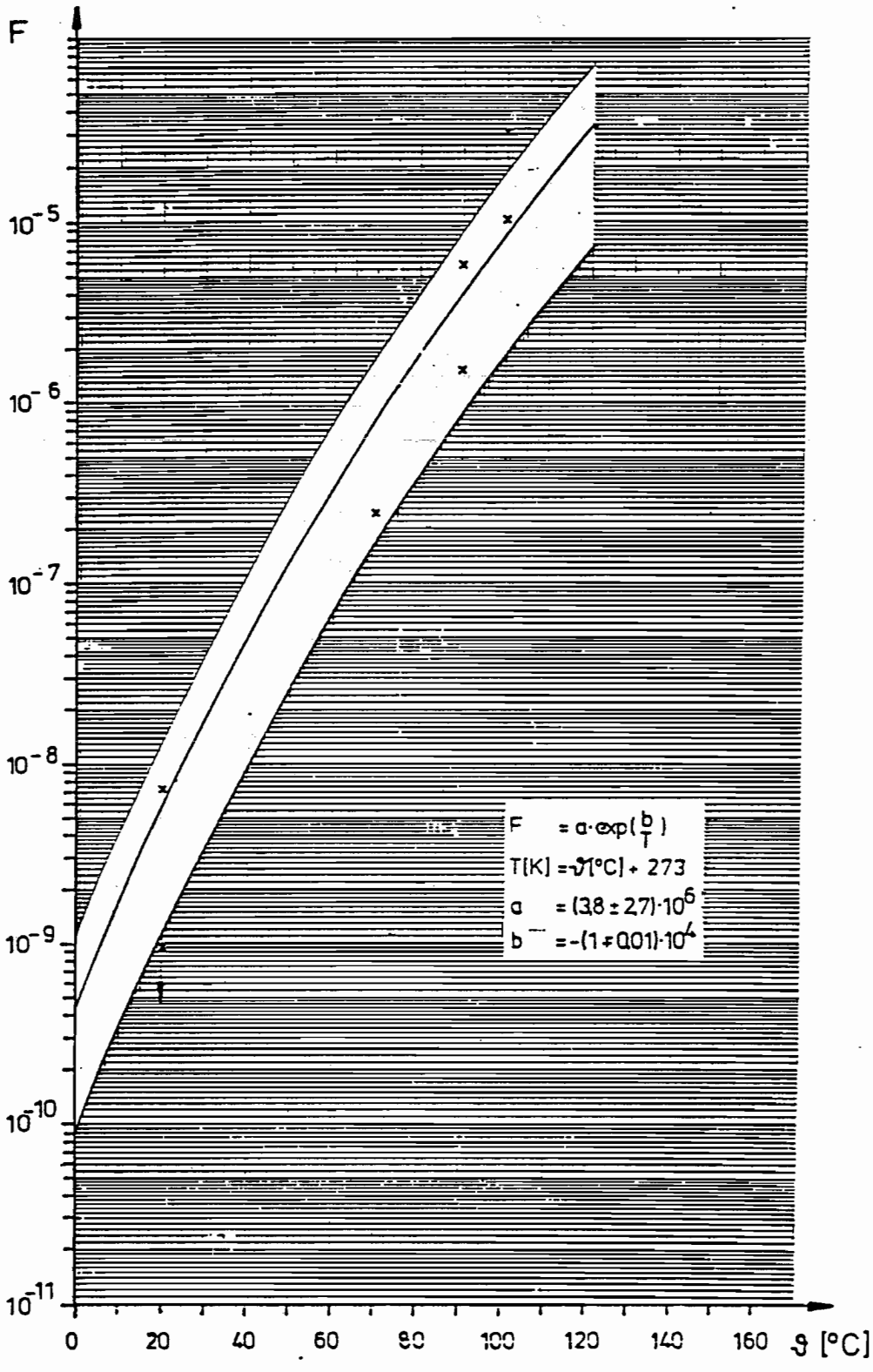

Figure 31 Regression law for entrainment from non-boiling solutions proposed by (61)

for the different boiling regimes:

$$E = C \cdot N^{0.5} \cdot d^{-1} \cdot v^{*3}$$

where C is a numerical value and the other terms the same as explained above. The decrease due to the deposition effects is given by

$$E \sim \exp (-c \cdot h / D),$$

where c relates the gas velocity with the deposition velocity and h and D are the height above the pool and the hydraulic diameter of the evaporator vessel respectively.

The experimental data to which these relations are fitted show scattering of nearly one order of magnitude. Especially for the conditions of lower gas flow, the available entrainment data base is not as copious as it is for more typical operating conditions of evaporators. The entrainment predicted by the given relations will therefore include some error but will at least give the right order of magnitude, as can be seen by the comparison of theory and measurement in (59).

Below boiling point no mechanistic physical model is given in the literature. Dorst (60, 61) has proposed an exponential law for aerosol release from aqueous solutions as a function of the inverse temperature. Such behaviour is usually found in systems obeying Boltzmann's law.

The pre-exponential and exponential constants are empirically adapted to the experimental results of (28). The regression law is in agreement with the measured points within a bandwidth of roughly one order of magnitude. The plot is shown in Fig. 31.

5. Review of the Data with Respect to Their Applicability to LWR Accidents

The evaluation of the existing data on entrainment and resuspension requires clear statements about 'realistic' values of the known main parameters of influence on these phenomena.

The main parameters of particle resuspension are basically not known. Influence of temperature has been presumed by Schütz (14) but was not verified by his experiments. There may be influence from the rate of boil-off, as is the case with the entrainment of droplets, because of a possible mechanistic link between these phenomena. The main parameters of droplet entrainment are known. Decisive influence comes from the vapour velocity, which can be separated into vapour generation rate and evaporation area. The evaporation rate in units of volume/time is influenced by the density of the generated steam, which depends on the temperature and pressure in the containment. The evaporation area may be estimated from the possible sump volumes by simple geometric relations. Further, the geometric conditions of the vapour space have to be considered.

Representative values for the containment temperature are in the range from 100 to 150^{o}C, corresponding to pressure of 2 to 7 bar partly due to incondensible gas content and dependent on the accident scenario. Evaporation rates are assumed to be initially of the order of 5 kg/sec and falling during the accident. From possible sump volumes of 100 to 2000 m^3 evaporation areas between 167 and 700 m^2 are calculated, assuming the form of a section of a sphere of 56 m diameter, which is the containment diameter of the German Biblis B reactor, the plant cosidered in the German Risk Study (2). This diameter is at the same time a measure for the vapour space height of the evaporation system. An important question concerning the evaporation area is whether the evaporation takes place uniformly on the total area or is restricted to a smaller area - say above the molten core - which may have a cross-section of 40 m^2. The latter is regarded to be more realistic than uniform evaporation. With the

assumptions given above, vapour velocities are calculated in the range up to 13 cm/sec for a restricted evaporation area.

It is assumed that special attention should be given to the process of despressurization of the containment after its overpressure failure because of higher boil-off rates and a faster exhaust of the containment atmosphere to the environment. On the other hand recent calculations of the conditions in the containment show that considerable time is needed for the depressurization which leads to relatively unimportant additional boil-off due to the overheated sump water. Assuming a containment leak of 300 cm^2, it takes about half a day, giving an additional boil-off rate of 1,5 kg/sec from a sump of 500 m^3 (62).

The sump itself contains an aqueous solution of boric acid. The boric acid concentration may be of the order of 1 % at the beginning of the evaporation (roughly 2000 ppm B in the nomenclature of reactor engineering and essentially constant as long as the containment keeps its integrity and the leaked amount is small compared to the inventory of water. After depressurization the water losses lead to slow drying out of the sump. Consequently the concentration of its solids content will increase up to the solubility limits at the boiling temperature. At the end of this process considerable changes of surface tension, viscosity and density will occur. Further influences may result from the aerosol content of the sump. The total aerosol mass released from the core is taken as 3.5 tons, mainly insoluble metallic and oxidic particles of silver, fuel and structural materials.

Entrainment

The measured values of entrainment have been plotted in Fig. 32. It is seen that the change in the slope of dE/dv_{gas}, where E is the entrainment, and v_{gas} the gas velocity in m/sec, occurs at approximately 15 cm/sec, as is known from the theory, and that extrapolation

from the data obtained under high gas velocities would not be justified. The range of gas velocities below 15 cm/sec, which is most important for evaporating reactor sumps, is shown separately in fig. 33. There we see a considerable scatter of the data and an increasing slope of the curves with decreasing gas velocity. The data reported by Heger and by Mishima were obtained at undersaturated vapour conditions, those of Shor under high pressure and some of Garner's measurements on a foaming evaporator. If these are removed, fig. 34 is obtained. The remaining data, which refer to saturated vapour conditions, are represented within a scattering bandwidth of half an order of magnitude by the equation

$$E = 3 \cdot 10^{-6} \cdot \exp (31 \cdot v_{gas}).$$

The residual scatter of the measurements is likely to be due to the use of different apparatus which means different vapour space height, surface to volume ratio and sampling position, which are known to influence the measured entrainment values.

The measured entrainment is in rough agreement with the theory for the region of discrete steam bubble flow (59) up to steam velocities of 7 cm/s but for the region up to 15 cm/s, which turned out to be most important for revolatilization of fission products, no appropriate description by theory was found. The theory for entrainment in the intermediate gas flux region, which is fitted to experimental findings at higher gas velocity, would predict considerably lower entrainment. This can be expected if measurements done there are compared with low velocity data as has been done in fig. 32.

From fig. 33 also the influence of some varied parameters is seen. The entrainment under a pressure of 22 bar was higher than at atmospheric pressure by a factor of 5 - 10. Since this pressure is far higher than that expected in reactor accidents, it is concluded that no important

effects of pressure may be expected. The effect of the undersaturated steam conditions is very strong. The enhanced entrainment may be due to drying of the generated droplets with the consequence that they will be transported more easily to the gas space. Foam on the evaporating liquid has an astonishingly small effect. This seems to contradict the observation that the jet drops which carry most of the entrainment in evaporators are retained by the foam. A possible explanation is that this effect is compensated in part by an enhanced generation of small film droplets under foaming.

In sum, it is seen that measured values for the entrainment at low gas velocities are available but subjected to an uncertainty of about one order of magnitude if some differences in the experimental conditions are accounted for. Because of the difference between theory and measurement it is advisable for the moment to rely on experimental values only. Considerable additional uncertainty is introduced by effects of drying of the droplets because the size distribution of entrained particles is one of the main influence parameters for their subsequent transport and depletion behaviour.

The direct applicability of literature data to the core melt accident problem depends on how close the influence parameters match in both cases. In general, a good agreement is given with respect to temperature, pressure, vapour velocity and material composition because the literature has been selected under these criteria. No agreement is obtained by comparison of the geometric conditions. The vapour space height in the reactor building is at least one order of magnitude higher than in the biggest evaporator used in the experiments. This difference is very important, because the vapour space heights occuring in evaporators are within range of the ascent of the bigger droplets. This is clearly shown by Garner's droplet size measurements. The dominant influence of the big droplets is explicitly stated by the theory of entrainment (36, 59). Additional differences will be seen if one looks at the flow pattern of the steam. In an evaporator, the steam is accelerated in the steam line because of its smaller cross section compared with the boiler. Thus, a significant amount of the larger

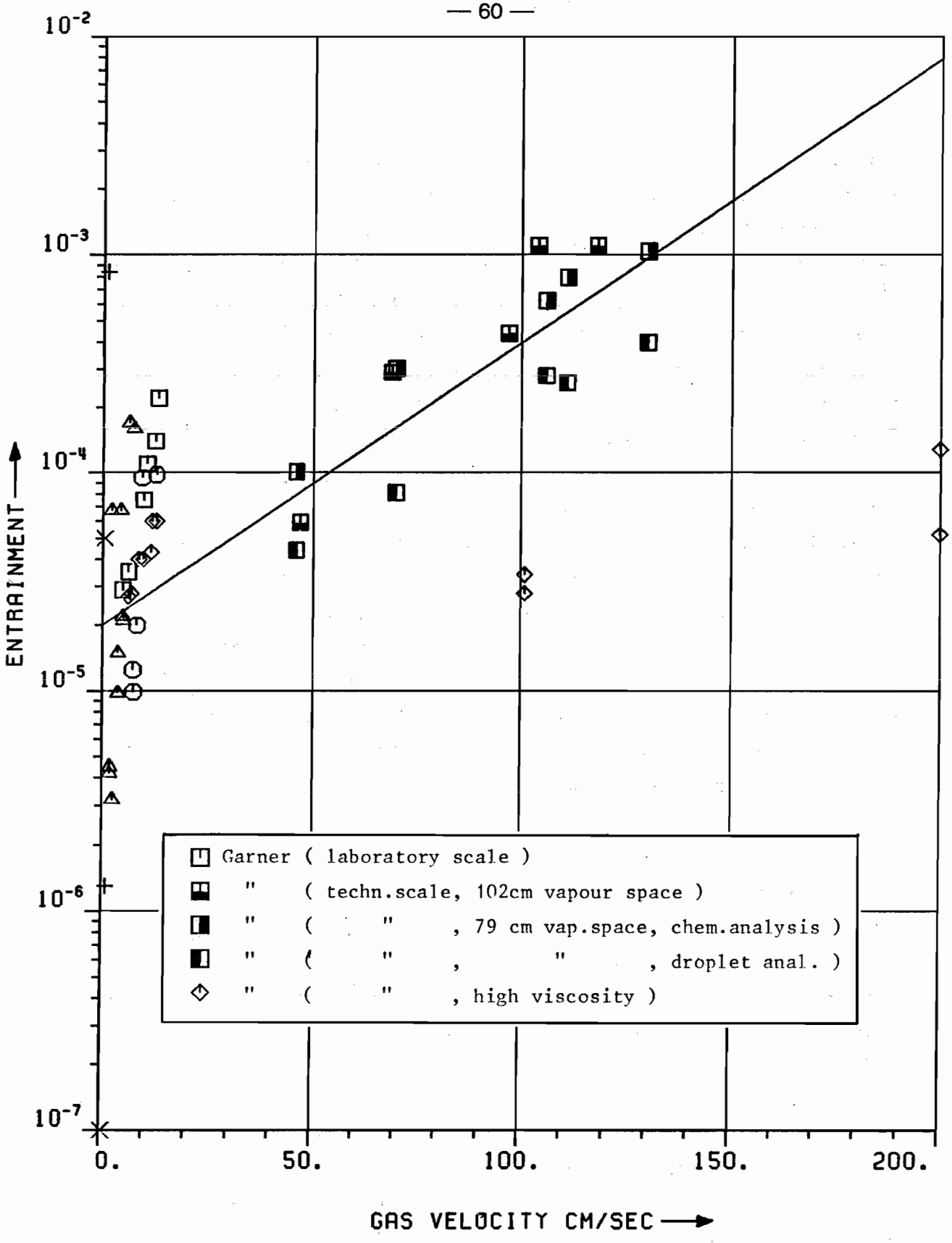

Figure 32 Entrainment data obtained by (28,32-35,37,38) at different gas velocity

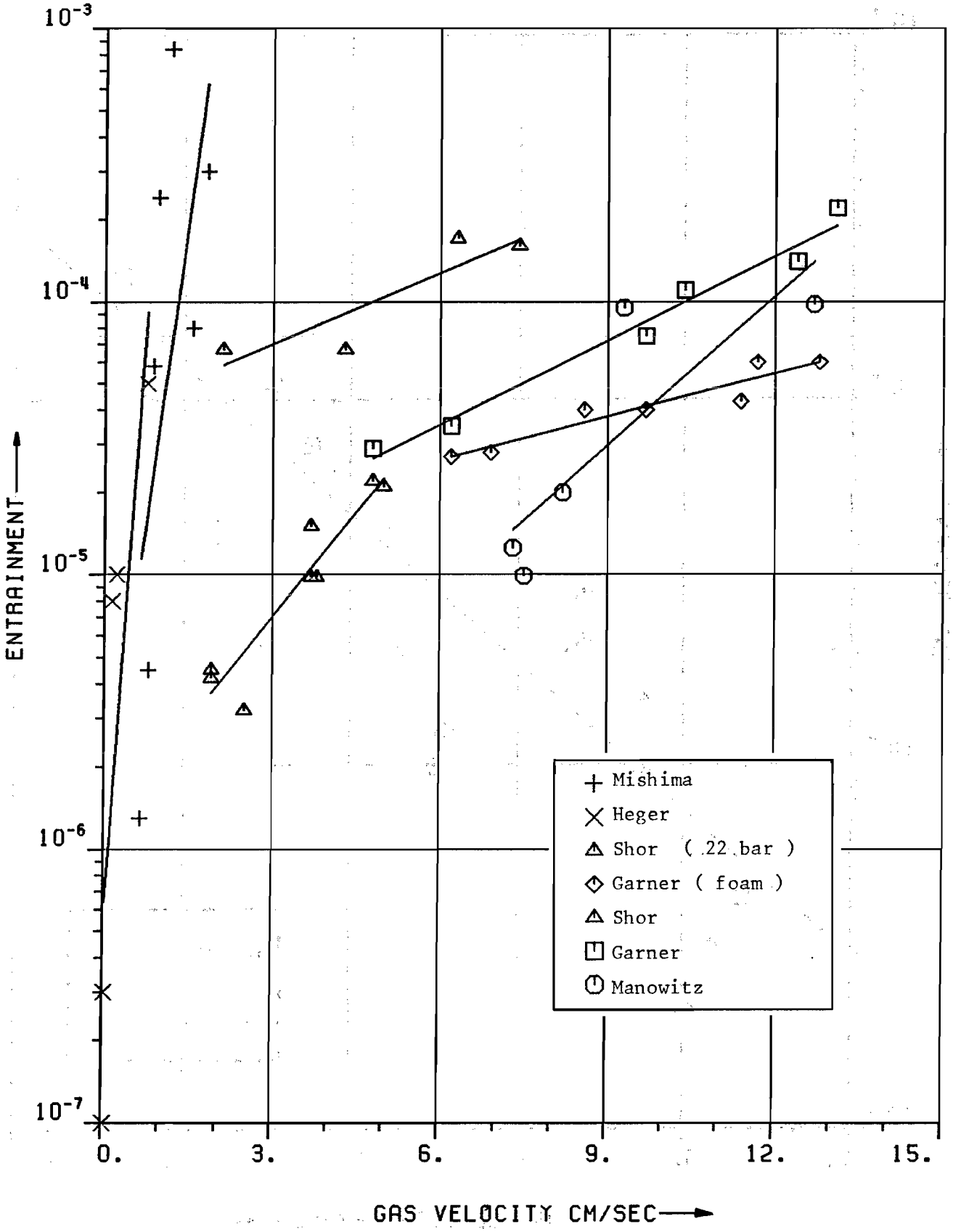

Figure 33 Entrainment data obtained at small gas velocity (28, 32-35, 37, 38)

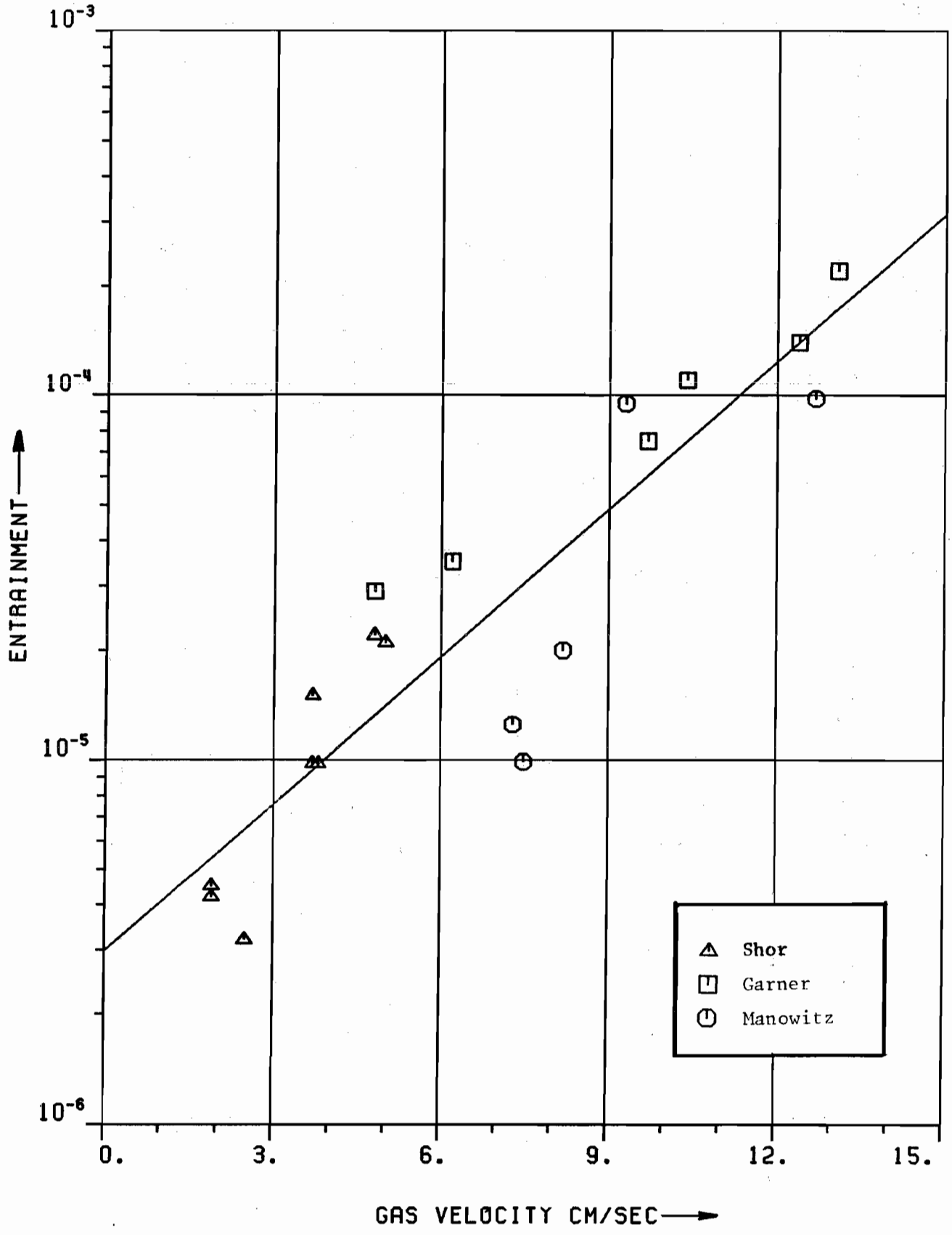

Figure 34 Entrainment measured under a vapour saturated atmosphere and near to 1 at

droplets will be carried out of the evaporator due to the high vapour drag on them. In a closed reactor building the vapour rises only due toconvective forces, with decreasing velocity. Also, in a open containment the residence time of the generated droplets will be very much greater than in an evaporator. This should lead to a more effective settling of the large droplets, which carry most of the airborne liquid. Thus, a possible conclusion is that for reactor application, the little film drops or evaporated large droplets are important but not the large ones as in evaporators. The fraction of film droplets is only of the order of a few percent of the total entrainment under ordninary boiling conditions. Calculation with the expression given by (59) for the zone of wall-deposition controlled entrainment yields values of about one percent of the measured entrainment as plotted in Fig. 27 at gas velocities above 7 cm/sec. At lower gas velocities much smaller fractions are calculated because of the third power dependence on the gas velocity. Measurement of the small droplets is not very reliable because of experimental difficulties, but indicates a mass fraction of few percent. Under foaming, a higher fraction of small droplets is expected, of the order of twenty percent (fig. 27) (34).

Detailed knowledge on the small droplets is not available. In general, all knowledge about important properties of bubble-induced droplets is related to jet drops or mixtures in which these predominate. The conclusion is that no judgement about enrichment of chemical species, effect of surface-active contaminants, etc. is possible.

Another important topic in the comparison of evaporators and the reactor containment is the question of steam saturation of the gas space. The containment atmosphere may be undersaturated in some regions or at some times, which should lead to a shift of the mean droplet size to smaller values. A quantitative prediction, however, is not possible on the basis of the existing data.

Resuspension

In this section, resuspension effects in the case of boiling or bubbled liquids are treated separately from effects in the absence of bubbles, since under the latter circumstances no mechanism is known.

Little data exist on the resuspension of particles from boiling or bubbled liquids. From the decontamination factors obtained in pool-scrubbing tests a value of $7,5 \times 10^{-4}$ results as an average of the experiments of Marble at 167 cm water depth (17). From the other experiments (19,20) higher resuspension, up to 2 %, is calculated. The value of $7,5 \times 10^{-4}$ is also obtained by recalculation of the sodium data reported by Schütz (14,15). For this calculation the release fraction of the uranium particles is related to the release fraction of the sodium pools, thus obtaining a particle release value which refers to complete evaporation and is higher than the inverse of the retention factor. This treatment implies time-linear particle release, contradicting Schütz's suggestion, that the release at full evaporation should not exceed the fraction measured at 10 % evaporation. It leads however to a reduction of data scatter and is in better agreement with the values reported by Berlin (9), which have been obtained under very similar conditions but with complete evaporation. Inversion of Berlin's retention factors, which refer also to simulated fission product particles, yields an averaged value of 9.8×10^{-3}. Further detailed analysis of the main parameters and other general interpretation is not possible because the lack of data.

Below boiling point data are available from sodium and water experiments by Schütz and Berlin, and are plotted in fig. 35 against the inverse temperature normalized to the boiling temperature of water and sodium. This type of plot has been chosen because of a likely dependence of the particle release on Boltzmann's law. Indeed, a temperature dependent release is seen, which obeys within a spread

of more than one order of magnitude the equation

$$\text{resuspension} = 1.2 \times 10^{-3} - \exp(3(T_b - T)/T),$$

where resuspension means the resuspended fraction at complete evaporation, and T_b the boiling temperature of the solvent.

The values used in the plot are Berlin's inverse retention factors and recalculated values from Schütz's data, which have been treated in the manner described above. Reference has been given to experimental data which are likely to represent the full extent of the particle release and not to suffer from possible retention mechanisms. Through this, and through manipulating Schütz's data an indefinite bias towards high release may be possible, but no conservatism in the choice of data was intended.

It can be seen that the resuspension in the vicinity of the boiling point will be in the region of 10^{-3}. No general difference between the water and sodium-related results is stated but this may be due to the lack of more water-related data. The influence of the evaporation rate on the release was also checked but no correlation found.

The application of the resuspension data presented in the literature to the situation of reactor accidents is hampered by the uncertainty about the mechanism of this effect. Measurements done below boiling point in aqueous and sodium systems suggest that there exists a mechanism independent of entrainment and of its main parameter, gas velocity. Also, if it is assumed that these experiments involved minor bubbling which might have gone undetected, the observed resuspension fraction of 10^{-4} or more is not in good agreement with entrainment fractions of 10^{-5} or lower at slow gas velocities unless considerable enrichment of the particles in the droplets is assumed. On the other hand, not assuming droplet-type resuspension would imply an independent mechanism for resuspension which may also be operative to an unknown extent under conditions of boiling.

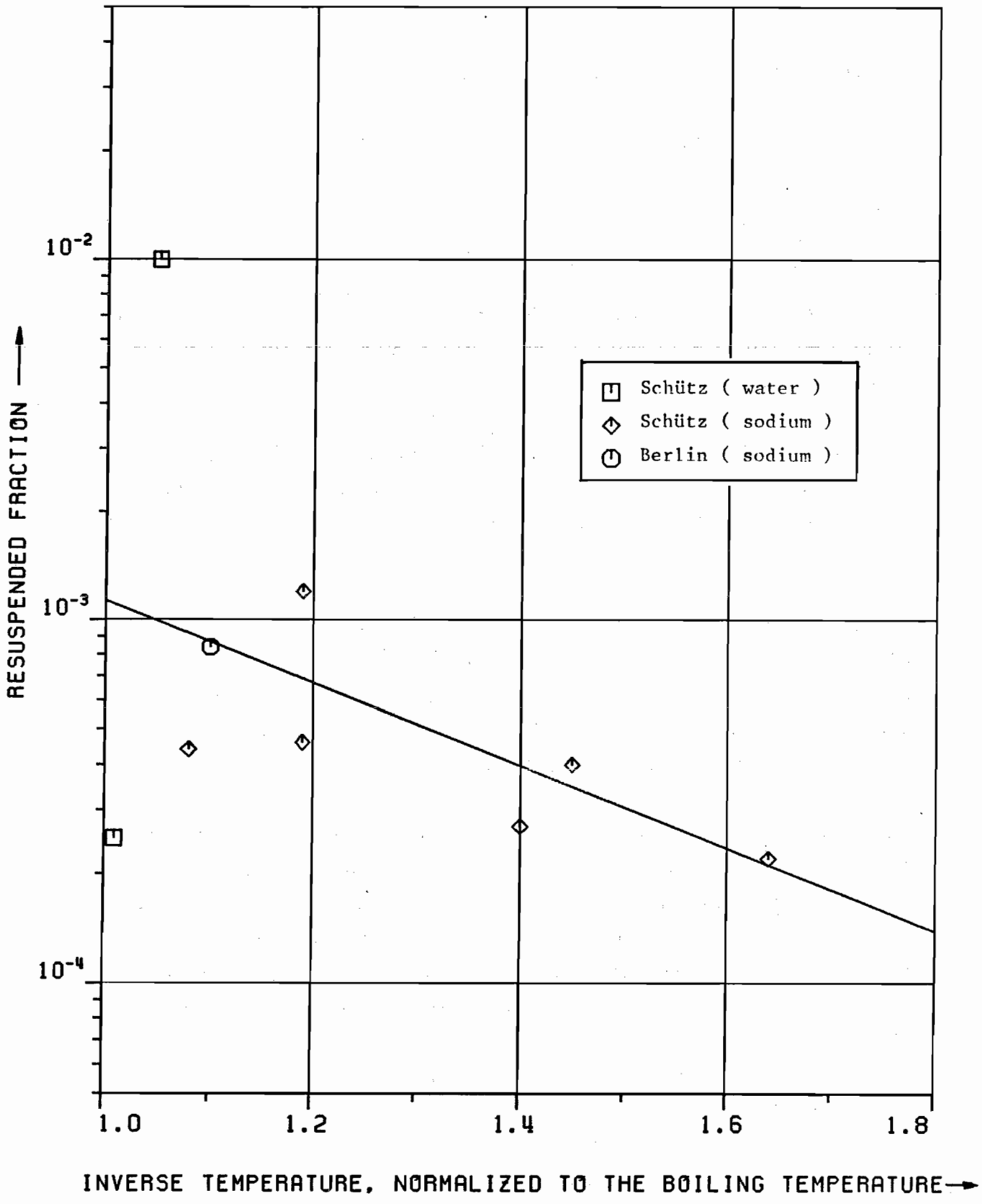

Figure 35 Integral resuspension of particles from non-boiling liquids vs. normalized inverse temperature (experimental data from (14,15,9))

Since such a postulated mechanism is not known but enrichment of particles has been observed, the best possible conclusion is that resuspension is due to entrainment type mechanisms. However, this has to be confirmed by further experiments evidence.

The applicability of the resuspension data obtained from boiling pools is now checked under the assumption of droplet transport. Gas velocity is the most important parameter for droplet carry-over. Gas velocity in sodium and water systems is not easy to compare because of much faster condensation of the evaporation sodium (63). It is to be assumed that this would lead to a lower release from sodium systems compared with water. Indeed, the Schütz's experiments with forced gas flow parallel to the sodium surface have shown higher releases, of the order of a few percent. But sodium fires which exhibit strong convective movement of the gas phase too, show no higher release than 10^{-3}.

Thus, considerable uncertainty has to be attached to even this central topic. Comparison of temperature, pressure and vapour space geometry, which act mainly via the gas velocity in water systems, is therefore dispensed with. The surface tension of sodium is higher than that of water, which may mean a better ability to enrich particles at the surface leading to higher release. Surface enrichment and surface effects in general have been stated by the researchers to be of importance to release, but there is no quantitative knowledge available. Ignoring nonlinear time behavior of the particle release in processing the data may contribute to fairly high release values. The only fact which gives some confidence in the transfer of the sodium data to aqueous systems is the agreement in the order of magnitude with the few water experiments which have been conducted. In conclusion, it is stated that the particle release from boiling suspensions may be of the order of 10^{-3} with an uncertainty of one order of magnitude in the direction of higher values and more uncertainty in the direction of lower ones.

The important question as to whether the resuspended particles are airborne as a result of an entrainment-independent mechanism or are carried by droplets should be regarded as unanswered by earlier experiments.

6. Impact of fission product revolatilization on the radiological source term

In order to check the influence of resuspension and entrainment of fission product aerosols from the sump on the radiological source term, calculations of the fission product release were performed with the NAUA code. The NAUA code (65) is an aerosol behaviour code which calculates the dynamic transport and depletion processes of aerosols in the condensing atmosphere of an LWR containment system during core melt accidents. The aerosol processes which are taken into account are Brownian and gravitational coagulation on particles as well as diffusiophoretic depletion. Aerosol sources can be chosen in an arbitrary manner. The calculation gives amongst other things the leakage of aerosols from the containment system which contributes to the radiological source term. As a basis for the calculations three different accident scenarios were taken from former (2) and current risk studies in Germany. The scenarios are LOCA with initially preserved containment integrity and late containment failure due to overpressure. This kind of accident scenario is the most frequent and moreover these cases are expected to be more sensitive to additional small released amounts of fission products than sequences with early containment failure.

The scenarios contain a set of time dependent data on the basic properties of the system - temperature, pressure, boiling rates and leak rates - which are used to calculate the generation of revolatilized fission product aerosols and are in part general input data for the NAUA-code. The NAUA-code calculates the deposition and leakage of the aerosols generated by the core melt and by the additional aerosol sources resuspension and entrainment. The aerosol

behaviour in the steel containment and in the annulus between the containment and the concrete shell is caluculated separately.

Accident scenarios I and II are characterized by a different amount of loss of coolant (600 and 2000 tons) from the primary coolant system and emergency core cooling systems into the containment. The long term pressure build-up leads to an enhanced leak rate when the design pressure is exceeded and to a depressurization of the containment through a leak of 300 cm^2 at the estimated failure point at 9 bar. Up to the depressurization, the water of the sump is circulated in the containment by evaporation and condensation. Once the containment has failed the residual time of the accident scenario is determined by the evaporation of the sump and its escape through the leak until the sump is dry. The point of "dryness", i.e.the end of vapour generation, was taken to be at about 95 % evaporation of the sump. It was assumed that the sump is boiled off mainly in the region above the core melt. The additional evaporation due to the pressure drop at depressurization was assumed to occur uniformly over the whole surface of the sump. The evaporation rate was taken as 5 kg/sec initially and falling during the accident to 3 kg/sec. From the evaporation area the evaporation rate and the thermodynamic conditions the entrainment was determined. The calculated vapour velocity was taken and the related entrainment read from fig. 34. Then, the fraction of 10 µm-droplets, the concentration of the sump and the drying of the droplets was corrected for and the aerosol source calculated in mass per second. The large droplets were neglected, since previous calculations with droplets larger than 10 µm had shown that these would not contribute to the aerosol source. The calculation of the drying of the droplets showed that at a relative humidity of 96 % or lower the 10 µm droplets will dry out so much (66) that their volume and diameter is governed by the precipitated boric acid in the droplet and not by the water content. Thus, not only the fission product content, but also the

diameter of the aerosols generated is dependent on the concentration of the sump and was corrected for during the accident. The droplets generated during the depressurization were assumed to stay as droplets of 10 µm and only their solids content was adapted to the actual sump concentration.

The density of the aerosol generated by entrainment was estimated from the density of boric acid with some corrections for the content of fission product particles to be 2 g/cm^3. This value was not varied with time nor for different accident scenarios. The density of the 10 µm-droplets was taken as 1 g/cm^3. The shape of all aerosols was assumed to be spherical. The generation rate, diameter, density and shape factors are the aerosol input parameters for the NAUA code.

The aerosols generated by the core melt were assumed to have a density of 5 g/cm^3 and a mean diameter of 0.6 µm, and to be sperical. The resuspended particles were not changed in their properties. In general, the resuspension rate was constant during the accident leading to the desired integral revolatilization by entrainment and resuspension.

Scenario III is similar in general but uses a modified failure mode of the containment after reaching the failure pressure. A progressively growing leakage up to 75 %/ day is assumed at constant pressure in the containment until the sump has evaporated and escaped through the leak. After the dry-out of the sump the overpressure is relaxed until atmosperic pressure is reached at the end of the scenario. This failure mode is considered as more realistic and is used in recent calculations for risk analysis purposes (64). It is an important feature of this scenario that it lasts longer than scenario I with a large leak. In this respect it is similar to scenario II which assumes a large sump volume of 2000 m^3.

The most important data of the scenarios are compiled in Tables 36-38.

Table 36: Scenario I (loss of 584 m^3 of coolant, containment leak of 300 cm^2 at 9 bar)

time ksec	temperature °C	pressure bar	mass of sump Mg	boil-off rate kg/sec	evapo-ration area m^2	concentra-tion factor (sump) -	leak rate vol%/ day	diameter (entrained particles) µm
0 - 350	120	3	506	5	40	1.00	0.25	2
350 - 450	150	7	406	3	40	1.25	2.5	2
450 - 500	120	3	401	3.2 + 1.3	40 287	1.26	890	10
500 - 520	100	1	176	3	40	2.88	600	3
520 - 540	100	1	116	3	40	4.36	600	3
540 - 550	100	1	56	3	40	9.04	600	4
550 - 555	100	1	26	3	40	19.5	600	5

Table 37: Scenario II (loss of 2084 m³ of coolant, containment failure at 9 bar by a leak of 300 cm²)

time ksec	temperature °C	pressure bar	mass of sump Mg	boil-off rate kg/sec	evapo-ration area m²	concentra-tion factor (sump) -	leak rate vol%/ day	diameter (entrained particles) µm
0 - 350	120	3	2006	5	40	1	0.25	2
350 - 450	150	7	1906	3	40	1.05	2.5	2
450 - 500	120	3	1901	3.2 + 3.8	40 642	1.06	890	10
500 - 600	100	1	1551	3	40	1.29	600	2
600 - 700	100	1	1251	3	40	1.60	600	2
700 - 800	100	1	951	3	40	2.11	600	2
800 - 900	100	1	651	3	40	3.08	600	3
900 - 950	100	1	351	3	40	5.72	600	4
950 - 980	100	1	201	3	40	9.98	600	4
980 - 1000	100	1	111	3	40	18.1	600	5

Table 38: Scenario III (loss of 584 m³ coolant, slow growth of a containment leak at constant pressure inside the containment)

time ksec	temperature °C	pressure bar	mass of sump Mg	boil-off rate kg/sec	evaporation area m²	concentration factor (sump) -	leak rate vol%/day	diameter (entrained particles) µm
0 - 350	120	3	531	5	40	1.00	0.25	2
350 - 450	150	6	435	3	40	1.22	2.5	2
450 - 550	160	7.5	388	3	40	1.37	25	2
550 - 600	167	9	301	2	40	1.76	75	2
600 - 650	167	9	204	2	40	2.60	75	3
650 - 670	167	9	107	2	40	4.96	75	3
670 - 690	167	9	68	2	40	7.81	75	4
690 - 700	167	9	29	2	40	18.3	75	5
700 - 750	167	9	10	0	-	-	60	-
750 - 950	150	6	10	0	-	-	30	-

In a first series of computer runs, scenario I (Table 36) was used. Runs were conducted

- without any revolatilization
- with strong entrainment only, and
- with strong entrainment and strong resuspension.

These runs were carried out in order to see the interaction of the aerosols from different sources and to obtain a reference release which enables us to judge the importance of additional effects. The comparison of the runs under different conditions of revolatilization showed only little interaction between the aerosols of different types. Some reduction of the smaller particles which stem from the core melt and are airborne by resuspension is seen in the presence of strong entrainment. But this effect is of little influence on the overall release.

The first and the last of the above-mentioned runs were compared with two subsequently conducted runs using scenario II and III each under similar conditions of strong revolatilization, as has also been done with scenario I. The aerosol leak rates of the four cases -

- scenario I without revolatilization ('reference'),
- scenario I under strong revolatilization,
- scenario II under strong revolatilization, and
- scenario III under strong revolatilization -

are shown in Figures 39-41 and the integral releases compiled in Table 42. In this series relatively high entrainment and resuspension rates were assumed to assure visible effects for all scenarios, because it was the predominant aim of these runs to determine the sensitivity of the fission product leakage on revolatilization in different scenarios and different phases of the accidents. The fraction of 10 µm-droplets was taken as 50 % of the literature entrainment value and the rate of resuspension chosen in a way that the integral revolatilization during all the accidents was about 10^{-3}.

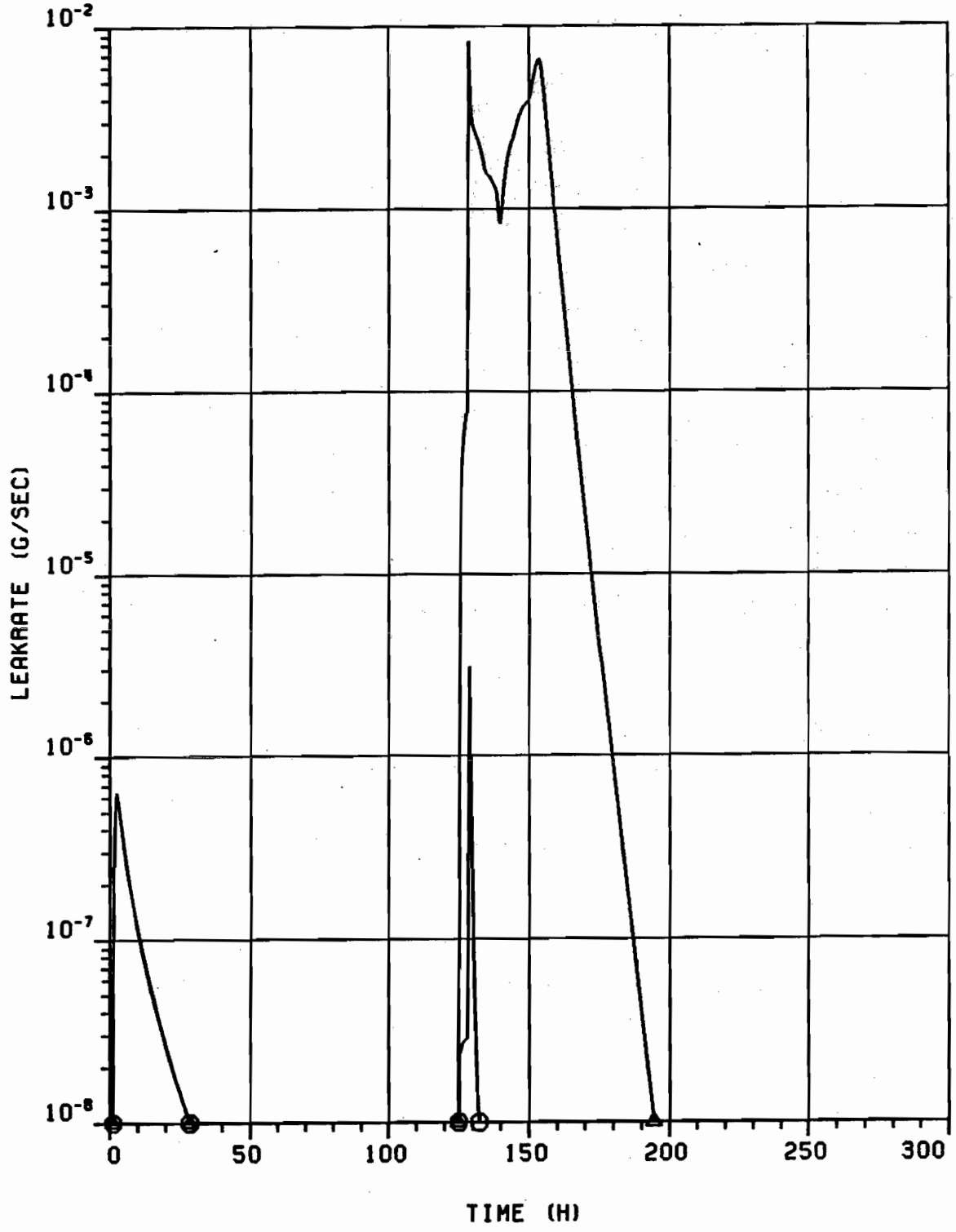

Figure 39 Aerosol leakrate from the annulus in the reference case (○) and under revolatilization in scenario I (△)

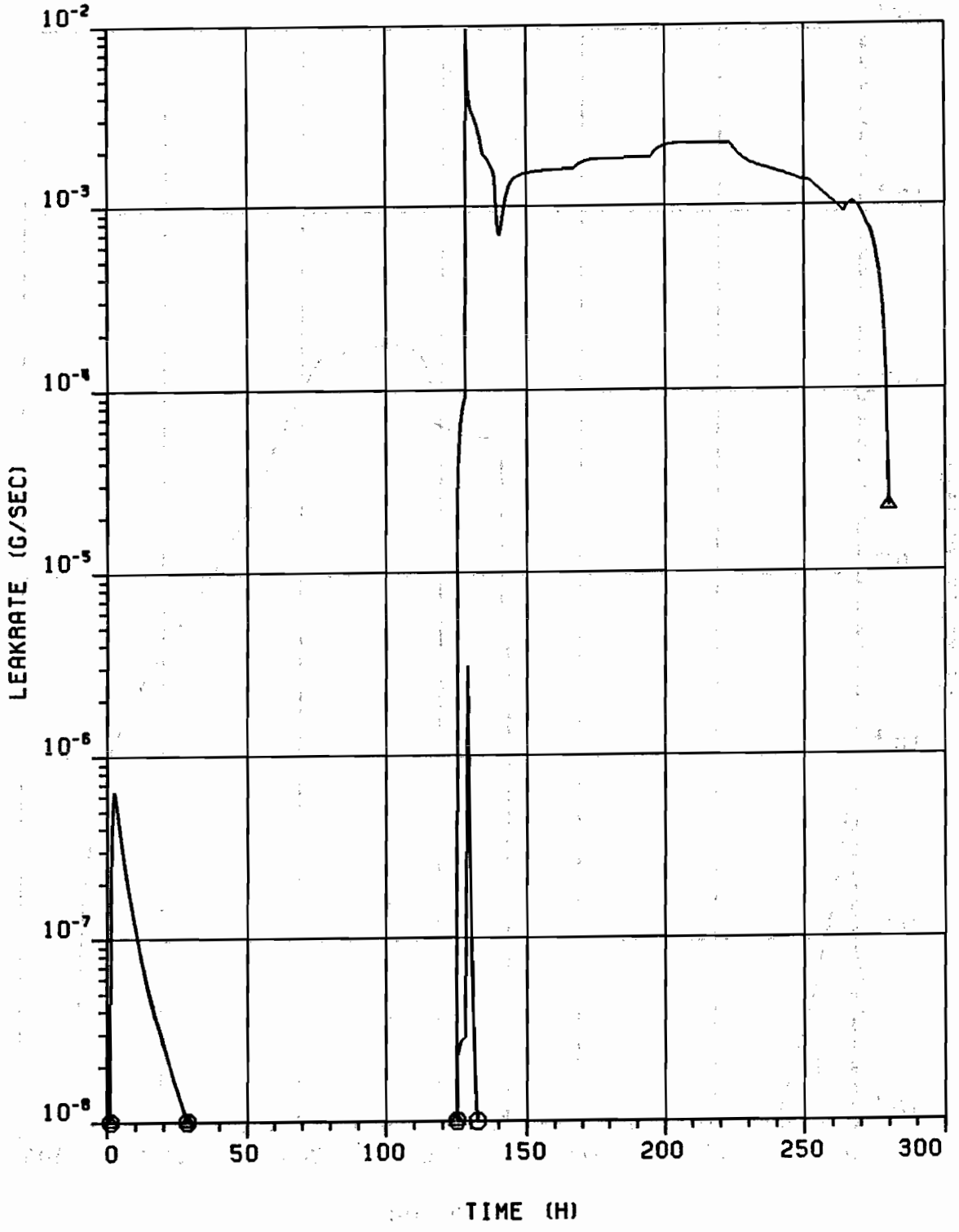

Figure 40 Aerosol leakrate from the annulus in scenario II (△) compared with the reference case (○)

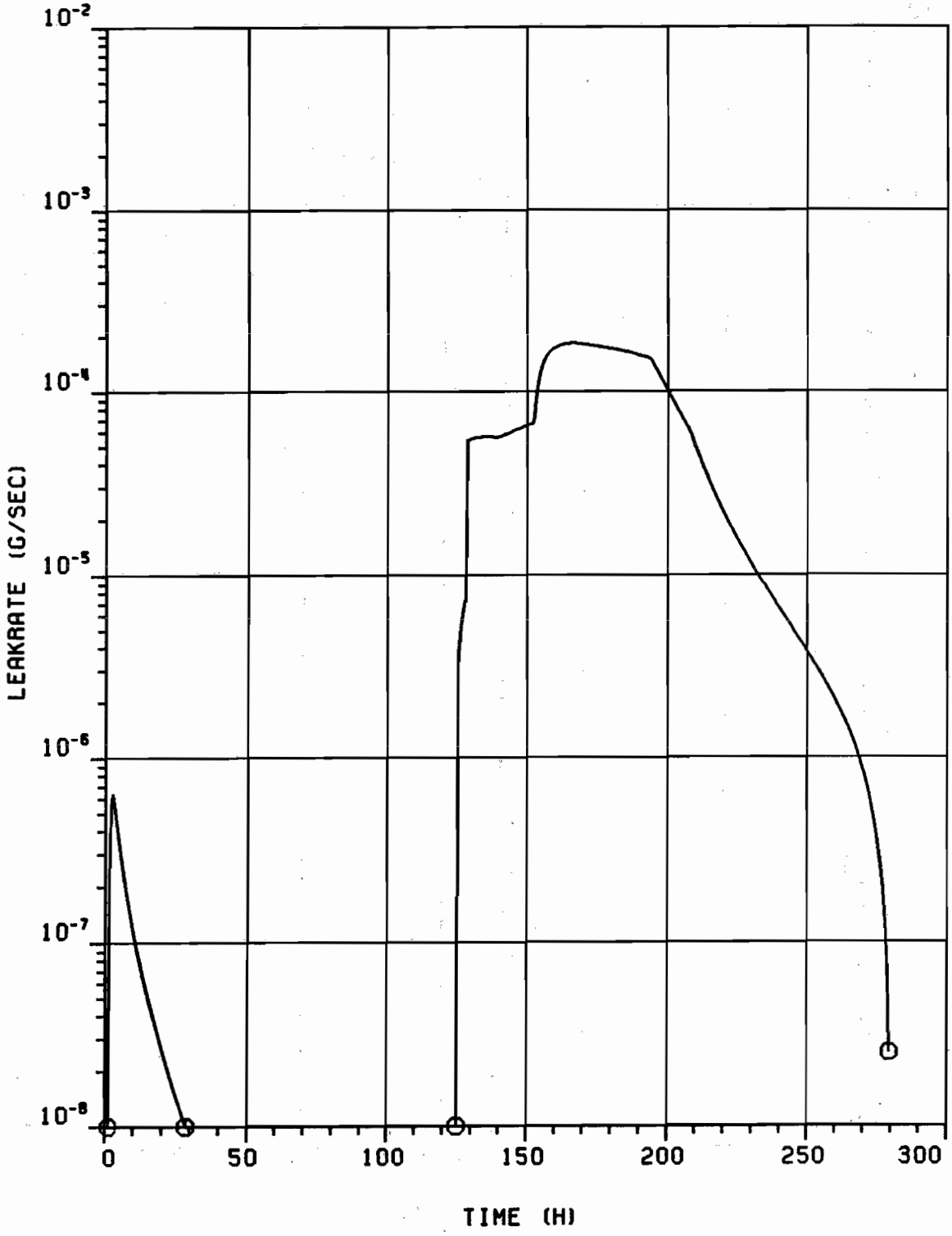

Figure 41 Aerosol leakrate from the annulus in scenario III

Table 42 Integral released fraction of fission products present in the sump at different accident scenarios

		Scenario I	Scenario II	Scenario III	Reference
release up to containment failure	containment		2.5×10^{-4}		
	annulus		1.1×10^{-5}		
	filters		1.1×10^{-8}		
release after containment failure by entrainment	containment	4.0×10^{-5}	4.0×10^{-5}	9.0×10^{-7}	($\sim 10^{-8}$)
	annulus	2.3×10^{-5}	2.2×10^{-5}	3.9×10^{-7}	5.6×10^{-9}
and by resuspension	containment	3.1×10^{-5}	2.1×10^{-4}	3.3×10^{-5}	(without
	annulus	1.6×10^{-5}	1.7×10^{-4}	1.4×10^{-5}	revolatilization)
sum of release to the environment		3.9×10^{-5}	1.72×10^{-4}	1.44×10^{-5}	1.66×10^{-8}

The comparison yields a very similar fraction of the fission product aerosols leaked from the containment before its failure (Figures 39-40). This fraction of 2.5×10^{-4} of the fission product aerosols released from the core was constant within one percent for all scenarios with and without revolatilization (Table 42). The conclusion is that revolatilization is of very little influence in this phase of an accident and the leakage from the containment is essentially due only to the original core melt aerosol generated at the beginning of the accident. The leakage is further reduced by aerosol processes in the annulus to a fraction of 1.1×10^{-5}. This fraction is filtered before it escapes to the environment by emergeny off-gas filters which have an efficiency of better than 99.9 %. Because of the filter effect, only a fractional amount of 1.1×10^{-8} will really escape to the environment. During the depressurization of the containment the filters are destroyed. This is the reason why any additional aerosol source after this time is relatively more important. In the reference case only a fraction of 5.6×10^{-9} is additionally released after the containment failure. Adding these two amounts the total escape fraction in the reference case is 1.7×10^{-8}. This fraction is taken as a base for comparison with scenarios under conditions of revolatilization.

By comparison of the leakage fractions of fission product aerosols compiled in Table 42 it is seen that under the somewhat pessimistic assumption which were made, the effects of entrainment and resuspension on the release to the environment are considerable in all cases. Further, it can be stated that resuspension should be of greater influence if both mechanisms of revolatilization exist to the extent assumed in the calculation. It should be noted that the sum of the two effects of revolatilization when given in the tables applies only to fission products which are subjected to both mechanisms. Dissolved fission products such as the important caesium and iodine species can be entrained only

The leakage of entrained particles was not influenced by the initial sump volume (scenario I and II), but was reduced by a factor of 56 in scenario III. The leakage of resuspended particles was low in scenarios I and III, but was very high in scenario II.

This complicated finding can be qualitatively explained as the result of two dominating influences. First, the escape of aerosols from any source to the environment requires a 'transport vehicle', i.e. a gas flow. Such gas flows are large after the containment failure, and fission product leak rates are proportional to the leaking gas flow. Second, the aerosol retention is governed by the particle size. On their way from the source to the environment particles can be depleted, depletion rates increasing with particle size. Since in the calculations resuspended particles were assumed to be smaller than reentrained droplets they are more persistent and in the longer lasting scenarios II and III the escaped fraction of resuspended particles contributes much more the leakage than the re-entrained fraction.

Besides leak rate and particle size the combination of other influences in the scenario also determine the amount of escaping fission products. So in many cases it is not possible to predict the influence of a single parameter change on the magnitude of the radiological source term. Only the calculations with the code can give reliable answers.

In the calculations discussed above the resuspension source rates were kept constant. In order to check the influence of a time-dependent resuspension source, which was suggested by Schütz (15), an additional calculation was performed. Using scenario II the resuspension rates were modified such that 80 % of the total resuspended mass were generated until 350ksec and 20 % thereafter.
The results were:

leakage before containment failure		1.1×10^{-8}
leakage after containment failure		
(by entrainment)	containment	4.5×10^{-5}
	annulus	2.2×10^{-5}
(by resuspension)	containment	6.2×10^{-5}
	annulus	3.8×10^{-5}
total leakage to environment		6.0×10^{-5}

As was expected, the leakage due to resuspension was reduced by roughly a factor of five and the total leakage by a factor of three compared with the standard scenario II (Table 42).

In the preceding calculations high source rates for revolatilization have been chosen because the main aim was to compare the effects of different accident scenarios. Since it is also intended to judge the absolute impact of revolatilization of fission products from the sump, a further calculation was conducted under conditions of revolatilization which are assumed to be closer to reality. The calculation was made on the base of scenario II, which assumes a sump volume of 2000 m^3 and containment failure by a leak of 300 cm^2 after 125 hours. This scenario is essentially identical to 'Kernschmelzfall 1' (CMA case 1) and release category 6 of the German Risk Study (2). The results are presented in more detail and will also show features which are common to all scenarios but were not discussed above. The rate of entrainment is known and given by the physical conditions of the scenario and cannot be chosen arbitrarily. Not as well known as the total entrainment rate is the important fraction of small 10 µm droplets. For the present calculation a mass percentage of 5 % was assumed which is adapted to the experimental findings of Garner (30) at low gas velocity (Figure 27). The integral resuspension was assumed to be 10^{-4} which is the lower limit of the

experimental findings. This choice was made because of the uncertain mechanism of the effect.

The results of the calculation are:

release before containment failure		1.1×10^{-8}
release after containment failure		
(by entrainment)	containment	4.4×10^{-6}
	annulus	2.2×10^{-6}
(by resuspension)	containment	1.8×10^{-5}
	annulus	1.3×10^{-5}
total leakage to environment		1.32×10^{-5} .

The time behaviour of the leakage is shown in fig. 43 and compared with the reference release. The results are qualitatively the same as before. Resuspension is more important than entrainment, essentially due to the assumed source rates but also due to the smaller size of the resuspended particles compared to the particles generated by entrainment. The retention of the re-entrained particles inside the containment is larger. The total release due to revolatilization effects after containment failure is much more important than the release before containment failure. This is also true if only the release due to entrainment is compared with the reference release.

According to the quantitative values it should be noted that some items have been ignored, which implies that the results obtained still include some conservatism, at least with respect to the effect of entrainment. The entrained droplets undergo deposition inside the reactor cavity. Further, the strong dependence of the calculated results on containment leak rates may lead to reductions when the leak rates after the containment failure are reduced to 'realistic' values.

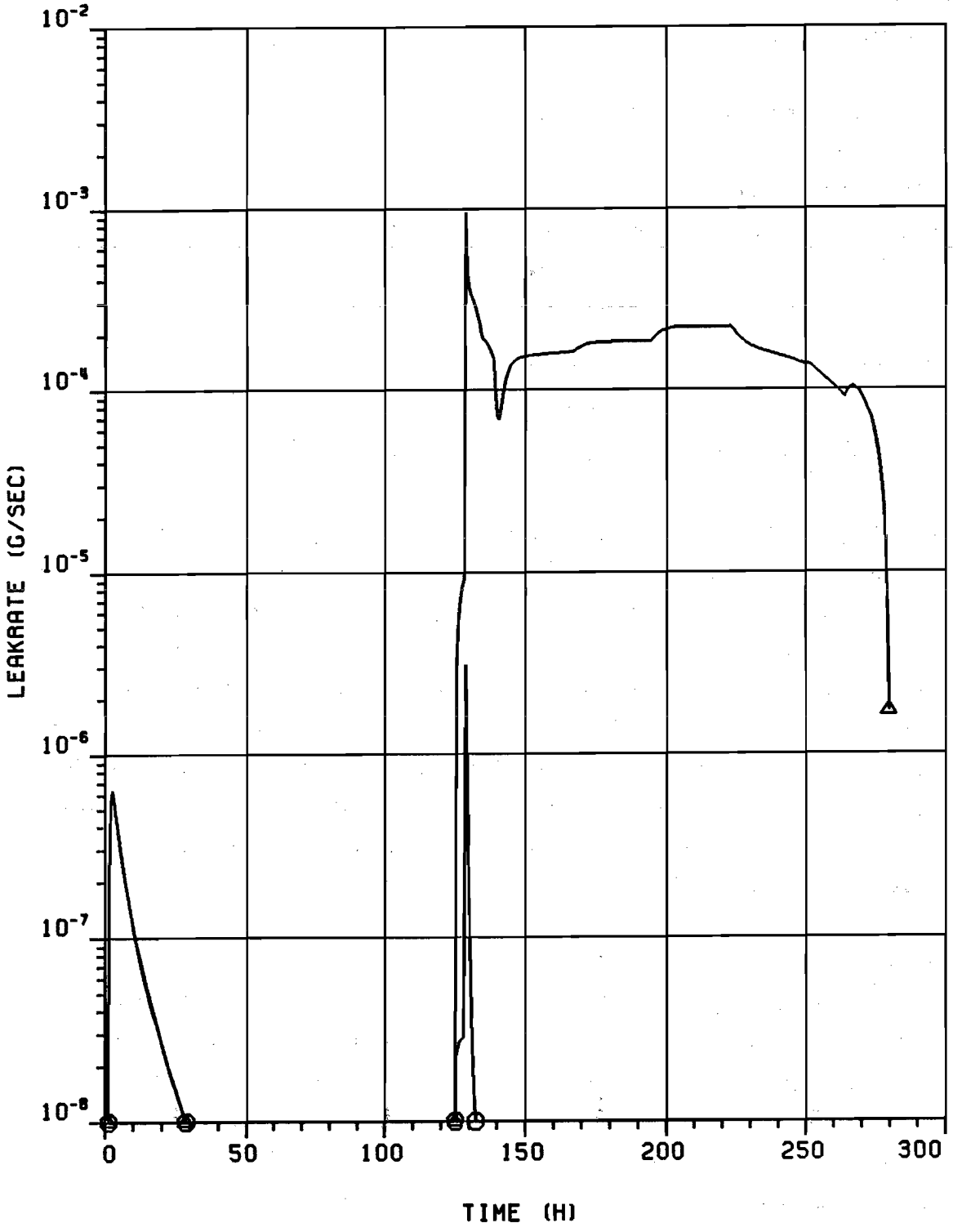

Figure 43 'Realistic' estimate of the aerosol release from the annulus in scenario II (Δ) compared with the reference case (O)

The simplified model for entrainment also involves some conservatism. The size distribution of entrained droplets cannot be obtained from literature data with the precision necessary for the application to accidents in LWRs. Changes in the fraction of 10 µm droplets influence the overall result very sensitively. This certainly requires further investigation.

So far only leakage values have been discussed. The NAUA calculations yield much more information which may be useful for the interpretation of the overall results. From these the airborne concentrations in the containment and in the annulus are shown in figs. 44-47. The NAUA code is capable of tracking individual aerosol species. Cs and Te have been chosen as representative materials of soluble and particulate fission products. Their time-dependent airborne concentration will now be discussed separately. Accident scenario II was used as well as the reduced revolatilization sources(fig. 43).

The airborne mass of caesium in the containment and in the annulus is shown in figs. 44 and 45. The qualitative time-behaviour shown there is typical also for the other scenarios.

The high initially airborne masses of core melt aerosol in the containment atmosphere is deposited during the first phase of the accident when the containment integrity is given. An equilibrium with the effects of revolatilization is reached before depressurization. Under enhanced leak rate due to increased pressure and under the depressurization this equilibrium is readjusted at a lower aerosol concentration inside the containment and more aerosol is leaked into the reactor building. During the important phase of boiling-off of the sump water when most of the Cs-leakage occurs the airborne mass is nearly constant over a long time and governed by the equilibrium of revolatilization, deposition and leakage. At the low

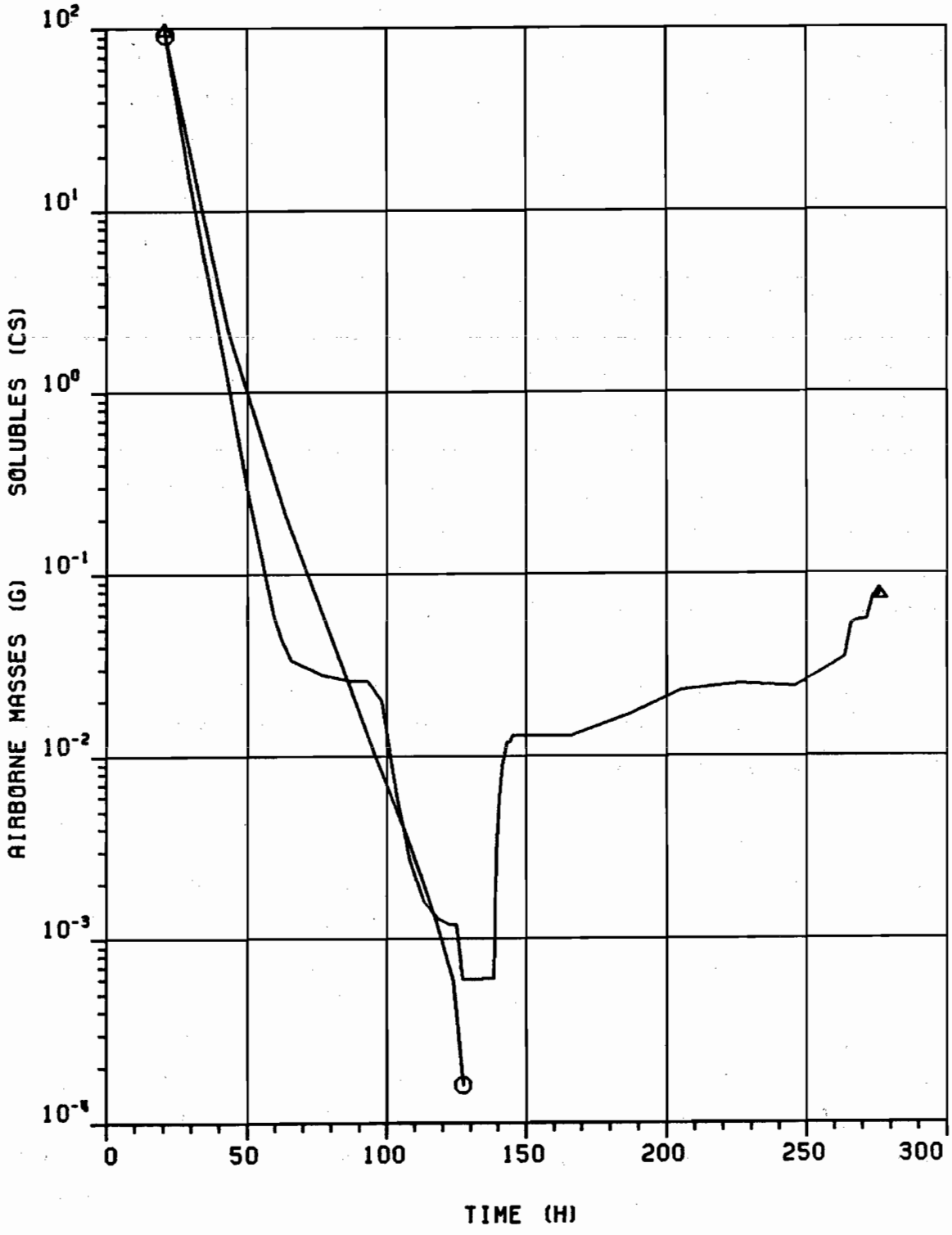

Figure 44 Mass of soluble fission products airborne in the containment in scenario II (Δ) compared with the reference case (○). The quantitation refers to cesium.

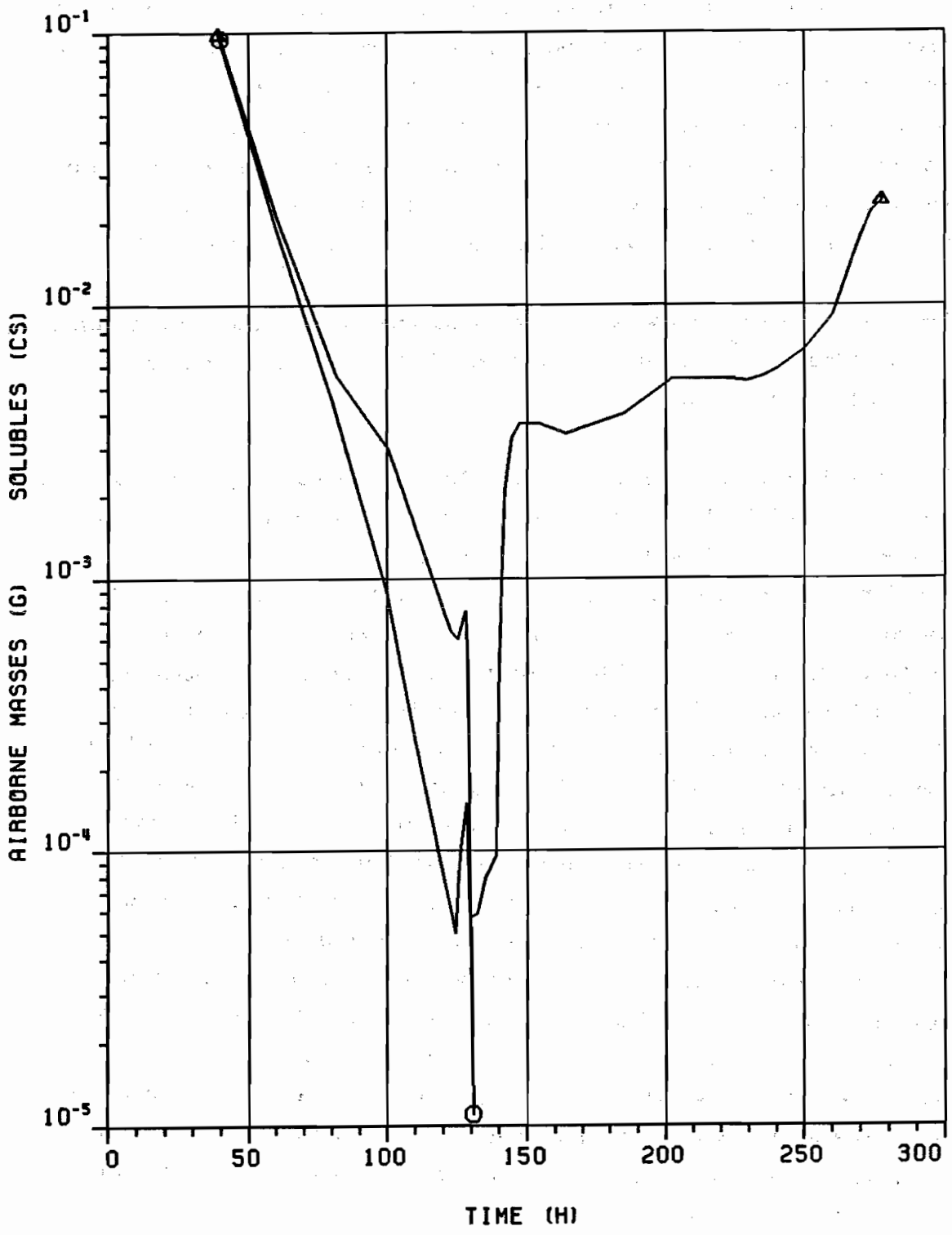

Figure 45 Mass of soluble fission products airborne in the annulus in scenario II (△) compared with the reference case (○). The quantitation refers to cesium.

aerosol concentration given her the equilibrium value is approximately proportional to the assumed source rates of revolatilization, because the aerosol interaction processes are weak. This is the reason why direct proportionality of the revolatilization source rates and the integral release is observed for the same scenario. This can be seen by comparing fig. 40 with fig. 43, belonging to the same scenario II with variation of the revolatilization effects by a factor of ten.

The mass airborne in the annulus follows that in the containment with little time delay, because the volume of the annulus is smaller than the containment volume.

The behaviour of the airborne particulate tellurium (figs. 46 and 47), which is revolatilized also by entrainment but predominantly by resuspension, is similar to that of caesium, which is entrained only. The final increase of the Cs mass generated by entrainment, which is due to the concentration changes in the sump, is not observed to that extent for insoluble Te particles. It should be noted that the airborne mass of tellurium is higher than that of caesium for long periods during the accident. The observed shift in the relative importance of individual nuclides for the radiological source term is due to the separation of soluble and insoluble fission products which was assumed for the present calculation. Soluble fission products were assumed to dissolve completely in the sump and to be re-entrained only. Insoluble particles are re-entrained too, but are revolatilized predominantly by resuspension, because of the higher source rate of this effect. This was done rather for methodical separation of the single effects than with the intention of physical modelling. The true extent of this potentially important effect was not studied in detail. The leak rates of caesium and tellurium are compared in fig. 48. From this it can be seen that the resuspended Te particles are more important

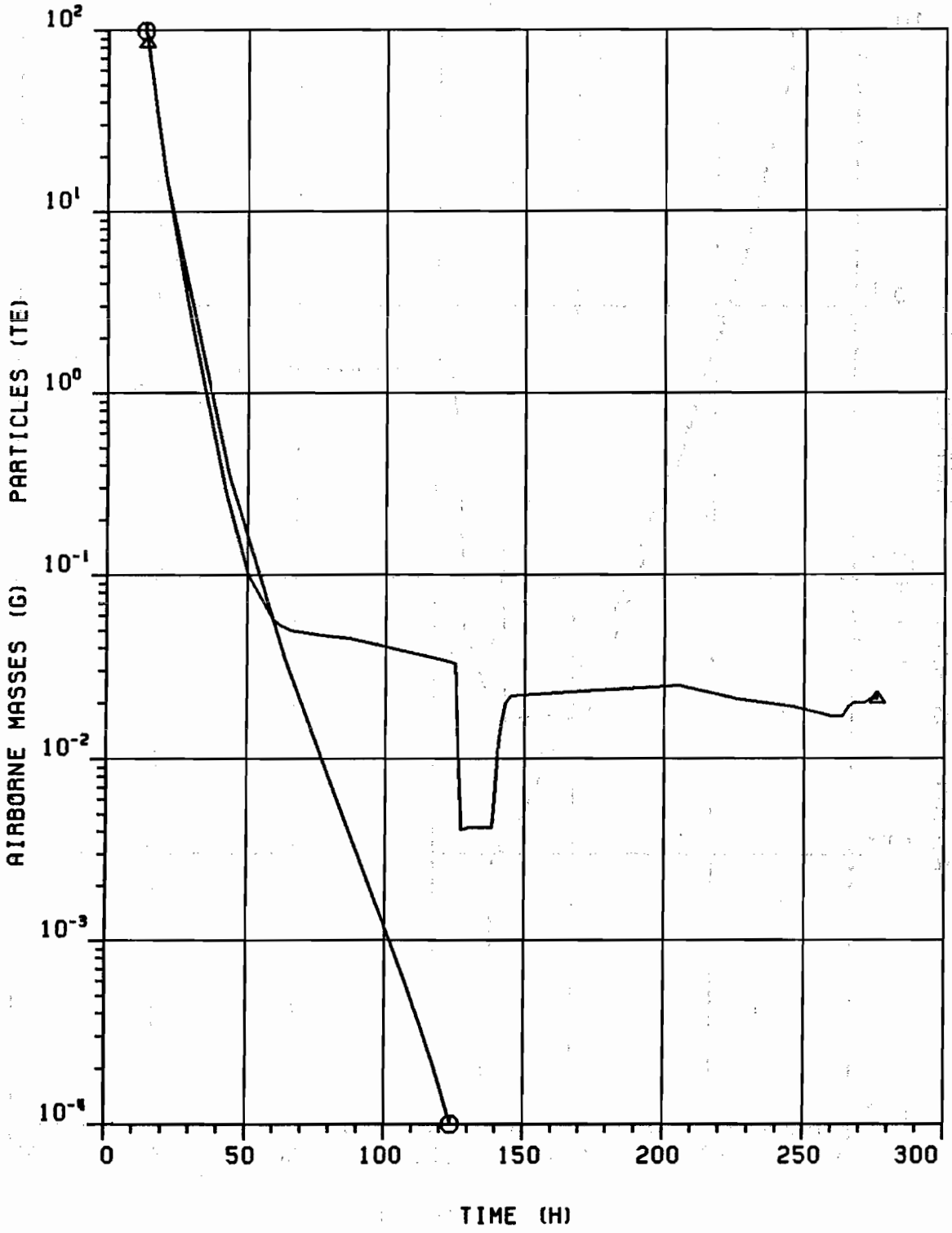

Figure 46 Mass of the insoluble fission product tellurium airborne in the containment in scenario II (△) compared with the reference case (○)

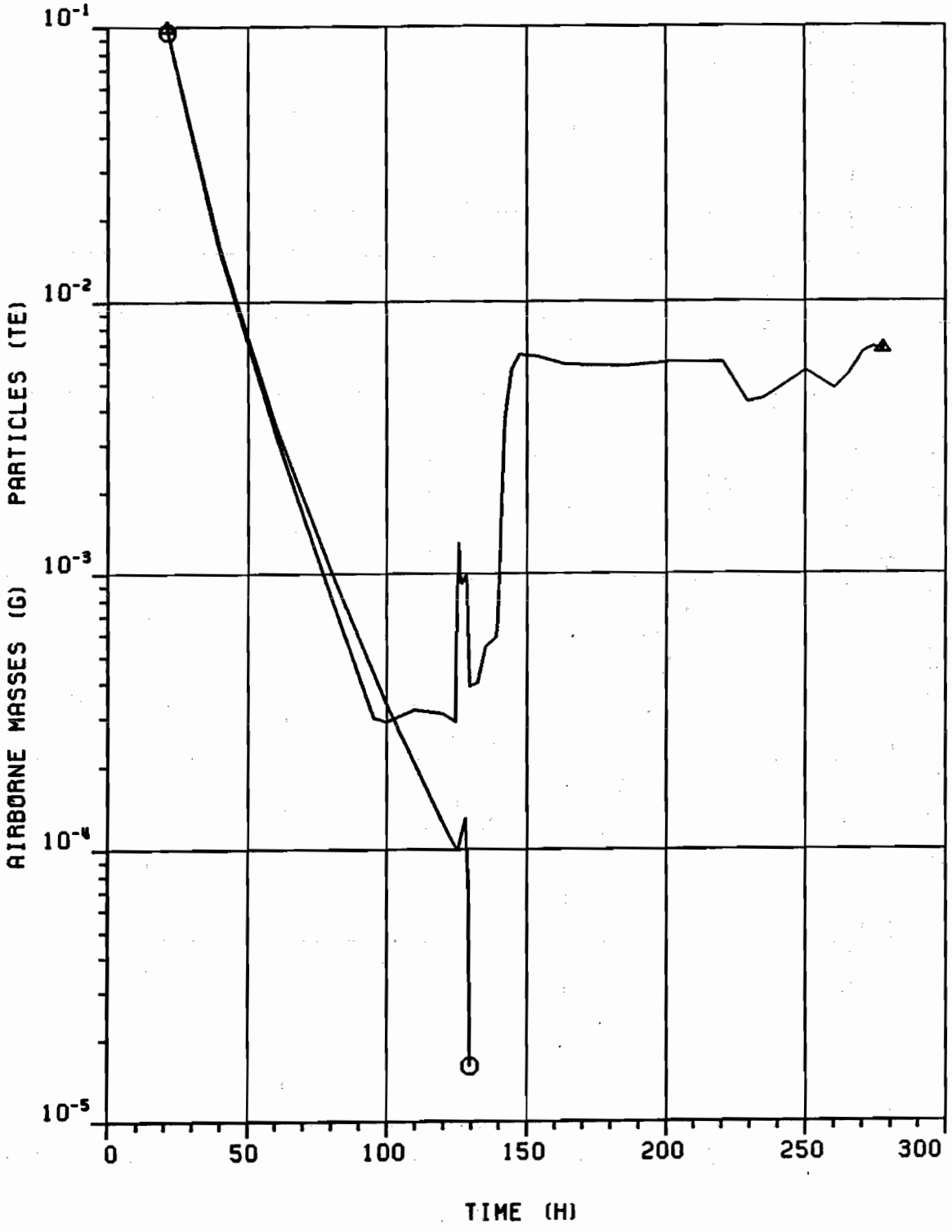

Figure 47 Mass of the insoluble fission product tellurium airborne in the annulus in scenario II (△) compared with the reference case (○)

during the earlier part of the boil-off phase while the entrainment of Cs is more pronounced during the later part when the sump is very concentrated. The integrally leaked amount of caesium (soluble fission products) and tellurium (insoluble ones) is similar. Comparison of fig. 48 with fig. 43 shows that most of the leaked mass in fig. 43 was boric acid. The boric acid mass is attached to the entrained fission products only and results in a different behaviour of the soluble and insoluble fission products.

To sum up:

The fission products may be revolatilized from the sump by droplet transport and perhaps by an unknown additional mechanism of resuspension.

- The re-entrainment of droplets from the sump yields particles of boric acid of a few µm in size which contain soluble and insoluble fission products according to their concentration in the sump. During an accident roughly a fraction of 10^{-4} of the fission products in the sump is re-entrained, but only a fraction of 10^{-6} will reach the environment under the assumptions which were made in the calculations. If some sources of conservatism are evaluated, which are inherent in the incomplete modelling, a best estimate of the releases during the later phases of an accident is obtained in the same order of magnitude as the releases during the early phase, which have been the result of previous risk calculations. The particles generated by re-entrainment are subjected to gravitational deposition to a larger extent than the original core melt aerosol due to their larger particle size, and therefore their airborne and released amount is more sensitive to accident scenario features. Entrainment of droplets from a boiling liquid is a well known phenomenon and the residual uncertainty about its impact originates from the not well known fraction of little film droplets, from possible effects of enrichment or depletion of fission products

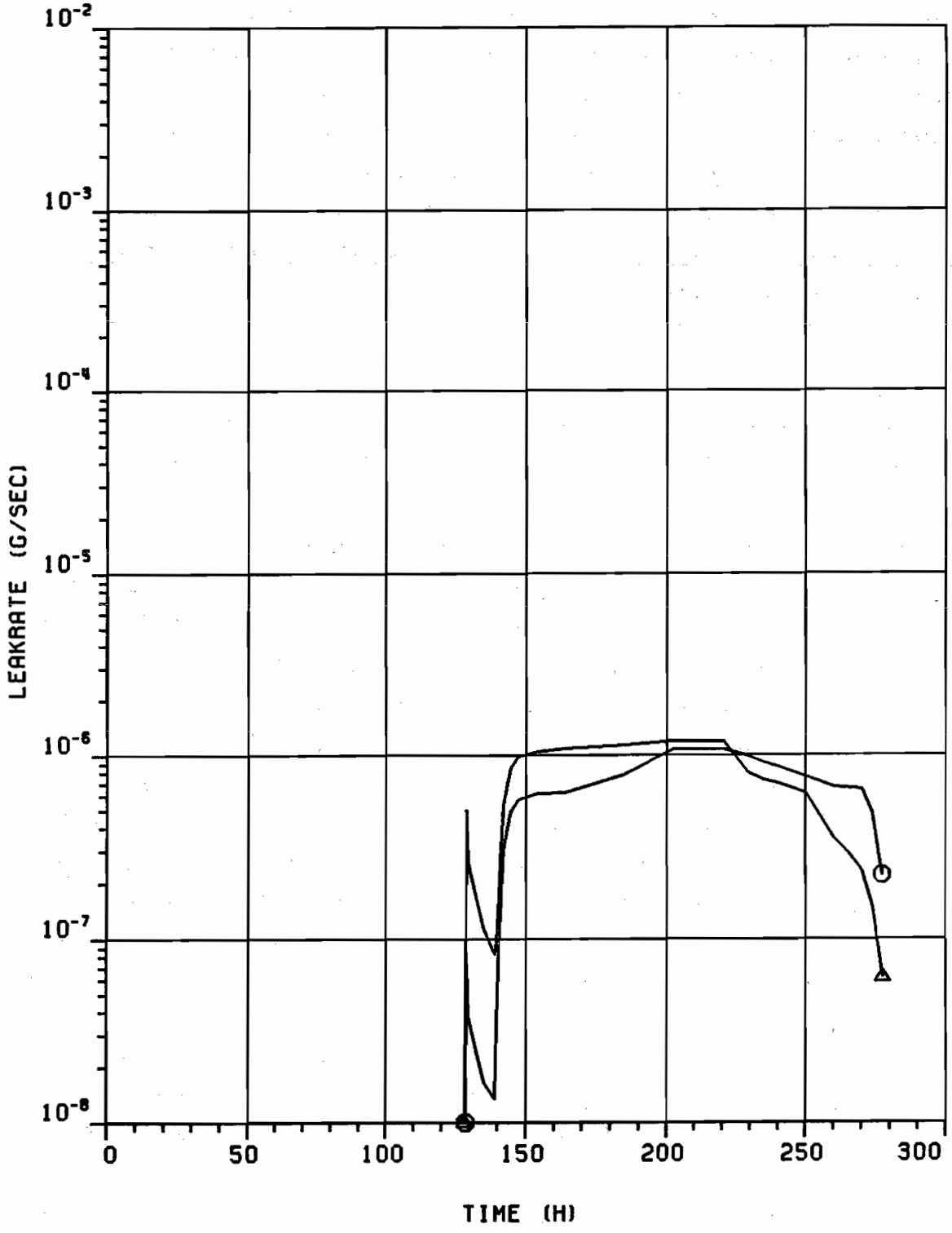

Figure 48 Aerosol leakrate from the annulus for a soluble fission product (cesium ○) and an insoluble one (tellurium △) in scenario II

in the droplets, and from the uncertainty about the relative humidity inside the reactor containment.

- The unknown independent mechanism of resuspension is assumed to yield airborne particles of the same size as the original core melt aerosol. It is likely that soluble fission products are removed or depleted in these, because they have dissolved in the sump before revolatilization. The range of values given in the literature for resuspension of particles from liquids would lead to a pronounced contribution to the total leakage in the late phase of the accident under the assumed accident conditons. Furthermore, the relative importance of several nuclides for risk assessment may be shifted. It has to be noted that this effect is subject to considerable uncertainty resulting from the general unavailability of detailed information.

7. Conclusions and recommendations

This study investigates the re-entrainment and resuspension processes of fission products from the containment sump of an LWR during core melt accidents. The contribution of these phenomena to the radiological source term is estimated. To this end a literature search was performed to gather available data on re-entrainment and resuspension rates, and parametric calculations with the NAUA code were performed to evaluate the fraction of revolatilized fission products that contribute to the radiological source term.

The following conclusions can be drawn:

- In the literature re-entrainment and resuspension have been investigated separately by different researchers with different aims and with different methods. Consequently the impression is given that we have two different phenomena to deal with. We do not support this, because then the resuspension phenomena would remain completely unexplained.

- Re-entrainment of dissolved material from aqeous pools is dealt with to a sufficient extent in the literature. Measured data show a clear dependence on the flow velocity of the steam. A qualitative understanding of the mechanism of re-entrainment is based on the process of bubble bursting at the water surface. The droplets generated from the bursting bubbles are carried away by the evaporated steam. From this picture the influence parameters are easily understood to be evaporation rate, surface area, size of the generated droplets and the geometry and saturation of the vapour space over the water surface. The latter influence of the vapour space is incompletely understood.

- Resuspension of particles is less well investigated. Information for aqueous systems is very scarce, a mechanistic model does not exist at all. The few existing data suggest that resuspension rates are higher than re-entrainment rates under identical conditions. The speculation that resuspension takes place via the same bubble-bursting phenomena as re-entrainment then leads to the immediate conclusion that particles in aqueous suspensions must be enriched at the surface. Such a surface enrichment has not been quantified for relevant aqueous systems.

- The applicability of re-entrainment and resuspension data to reactor accident analysis is impeded by the fact that no very many data are directly applicable to accident conditions, and that reliable models are not available. This problem is more severe for resuspension than for re-entrainment.

- Calculations of aerosol behaviour with the NAUA code show - when directly based on literature data - a strong relative increase in the radiological source term due to re-entrainment and resuspension effects as compared with earlier studies which neglected reentrainment and resuspension. It has to be kept in mind that even this increased source term is very low in absolute measures, because the accident sequence chosen for the calculation was a very low consequence scenario with late overpressure failure of the containment. The new calculations show that the additional contributions to the radiological source term occur after the containment failure at a time which was no longer taken into account in earlier calculations.

- Further calculations in which the literature data on resuspension and re-entrainment rates have been reduced by plausibility considerations as far as possible still resulted in a contribution of

re-releases to the radiological source term that was of the same magnitude as the direct release from the core. This again is valid only for the low-consequence scenario with late overpressure failure.

To sum up:

Re-entrainment and resuspension make the main contribution to the radiological source term in an accident scenario which is not risk dominant but by far the most frequent. The error latitude of this contribution, however, is very large due to incomplete physical understanding of the basic processes.

Based on these conclusions the following recommendations can be made for future research:

- The re-entrainment source should be measured more accurately. Under conditions that are applicable to LWR accidents the source mass rates and, more importantly, the droplet size spectra and chemical composition have to be measured. Detailed information on the dependence of this source on the geometry of the vapour space over the boiling pool should be gathered.

- The mechanism of resuspension should be investigated. It has to be determined whether an independent resuspension mechanism exists or whether particulates are also emitted from the sump by re-entrainment processes. At least in the latter case, surface enrichment factors have to be determined.

- On the basis of such experimental data a model for re-entrainment and resuspension sources should be worked out. This model should be generally applicable, but the exmphasis should be on the application to core melt accident conditions in LWRs.

- With the model a reassessment of the fission product leakage to the environment should be made, taking into account the new better-defined source model for re-entrainment and resuspension. The results will have to be compared to the present values of the radiological source term.

References

(1) NRC, "An Assessment of Accident Risks in U.S. Commercial Nuclear Power Plants", NUREG-75/014, WASH-1400, (1975)

(2) Gesellschaft für Reaktorsicherheit, "Deutsche Risikostudie Kernkraftwerke", TüV-Rheinland, Köln, FRG, (1980)

(3) NRC, "Technical Bases for Estimating Fission Product Behavior during LWR Accidents", NUREG-0772, (1981)

(4) Hoseman, Neeb, Wilhelm, "Neuere Bewertung der Freisetzung und des Transportes von Jod bei schweren Reaktorstörfällen", Jahrestagung Kerntechnik, Berlin, (1983)

(5) H. Bunz, W. Schöck, "The Natural Removal of Particulate Radioactivity in a LWR-Containment during Core Meltdown Accidents", ANS/ENS Topical Meeting on Thermal Reactor Safety, Knoxville, (1980)

(6) H. Bunz, W. Schikarski, W. Schöck, "The Role of Aerosol Behavior in LWR Core Melt Accidents", Nucl. Technol. 53, (1981), p.141

(7) W. Schöck, H. Bunz, "Best Estimate Calculations of Fission Product Release to the Environment for some PWR Core Melt Accident Sequences", Int. Meeting on Thermal Nuclear Reactor Safety, Chicago, (1982)

(8) OECD/ed., "Nuclear Aerosols in Reactor Safety", a State-of-the-Art Report by a Group of Experts of the NEA/CSNI, CSNI SOAR No.1, pp 45-46 OECD 1979

(9) M. Berlin et al., "Evaluation of the Sodium Retention Factors for Fission Products and Fuel", Int. Meeting LMFBR Safety and Operational Aspects, Lyon, (1982), poster session

(10) R.L. Koontz, D. Toppen, "Radionuclide Release from Burning Sodium", Safety Technol. Meeting on Radiological Assessment, (1975), ERDA - 56

(11) AI Staff, "Quarterly Tech. Progress Report, Nucl. Safety, Characterization of Sodium Fires and Fast Reactor Fission Products", AI - ERDA - 13166, (1975)

(12) J.L. Stakebake, H.N. Robinson, "Plutonium Release from Burning Sodium", Nucl. Technol. 33, (1977), p. 30-39

(13) "LMFBR Safety Program Annual Techn. Report, Gov. FY 1976 and 1976T", AI - ERDA - 13182, (1977)

(14) W. Schütz, "UO_2- und Spaltproduktfreisetzung aus Natriumlachen", KFK 3010, (1980)

(15) H. Sauter, W. Schütz, "Aerosol- und Aktivitätsfreisetzung aus kontaminierten Natriumlachen in Inertgasatmosphäre", KfK 3504, (1983)

(16) J.A. Quinn et al., "Breaking Bubbles and the Water-to-Air Transport of Particulate Matter", Chem. Eng. Sci. 30, (1975), p. 1177

(17) W.J. Marble et al., "Retention of Fission Products by BWR-Suppression Pool during Severe Accidents", Proceedings of the Int. Meeting on Thermal Nuclear Reactor Safety, NUREG/CP-0027, Vol. 2 pp 821-835 Chicago, (1982)

(18) D.M. Rastler, "Suppression Pool Scrubbing Factors for Postulated Boiling Water Reactor Accident Conditions" NEDO-25420, (1981)

(19) J.J. Hillary et al., "Iodine Removal by a Scale Model of the SGHW Reactor Vented Steam Suppression System" TRG report 1256, (1966)

(20) H.R. Diffey et al., "Iodine Cleanup in a Steam Suppression System", Conf-650407, 2 (1965) 776

(21) S. Jordan, Y. Ozawa, "Fuel Particle and Fission Product Release from LMFBR Core Catcher", Int. Meeting Fast Reactor Safety and Related Physics, Chicago, (1976), CONF 761001 - P4

(22) S. Jordan, Y. Ozawa, W. Schütz, "UO_2- und Spaltprodukt-Freisetzung aus heißen und siedenden Natriumlachen", Jahrestagung Kerntechnik, Mannheim, (1977) Tagungsband S. 323

(23) W. Schütz, "Natrium-Freisetzungsraten aus kleinen Natriumlachen bei aufgeprägter Konvektion", KFK 1277, (1977)

(24) H. Sauter, W. Schütz, "Aerosol Release from a hot Sodium Pool and Behavior in Sodium Vapor Atmosphere", CSNI Specialists Meeting on Nucl. Aerosols in Reactor Safety, Gatlinburg, (1980)

(25) S.L. Sutter, J. Mishima, J.W. Johnston, "Aerosols Generated by Free Fall Spills of Powders and Solutions in Static Air", PNL - 3786, (1981)

(26) H.J. Harding et al, "Aerosols Generated by Liquid Sludge Application to Land", EPA 600/1-81-028, (1981)

(27) K. Aurand, M. Fischer, "Emission luftfremder Stoffe aus Kühltürmen, Haustechnik, Bauphysik, Umwelttechnik 104 (1983) no.6,p.22

(28) J. Mishima, L.C. Schwendimann, C.A. Radash, "Plutonium Release Studies - IV. Fractional Release from Heating Plutonium Nitrate Solution in a Flowing Air Stream", BNWL 931, (1968)

(29) R.K. Hilliard, A.K. Postma, "Large Scale Fission Product Containment Tests", HEDL - SA - 2254 - FP, (1980)

(30) M.E. Witherspoon, A.K. Postma, "Leakage of Fission Products from Artificial Leaks in the Containment Systems Experiment", BNWL - 1582, (1971)

(31) A.H. Dexter et al., "Iodine Evaporation from Irradiated Aqueous Solution Containing Thiosulfate Additive", DP - MS - 76 - 19, (1976)

(32) B. Manowitz et al., "Entrainment in Evaporators", Chem. Eng. Progr. 51, (1955), p. 313

(33) F.H. Garner et al., "Entrainment in Evaporators", Trans. Instn. Chem. Engrs. 37, (1959), p. 246

(34) F.H. Garner et al., "The Size Distribution and Entrainment of Droplets", Trans. Instn. Chem. Engrs. 32, (1954), p. 222

(35) A.J. Shor et al., "Radioactive Carry-Over from Borax III and Test Systems", Nucl. Sci. and Eng. 2, (1957), p. 126

(36) G.C.K. Yeh, N. Zuber, "On the Problem of Liquid Entrainment", ANL-6244, (1960)

(37) R. Heger et al., "Bestimmung der Quellterme bei verfahrenstechnischen Operationen im Wiederaufarbeitungsprozeß", KfK-Nachrichten 14, (1982), No. 3, p. 143

(38) R. Heger, Th. Wäscher, "Charakterisierung der Aerosolemissionen im Behälterabgas einer Wiederaufarbeitungsanlage", Jahrestagung Kerntechnik, Berlin, (1983) Tagungsband p. 423

(39) R.F. Davis, "The Physical Aspects of Steam Generation at High Pressures and the Problem of Steam Contamination", Proc. Instn. Mech. Engrs. 144, (1940), p. 198

(40) D.M. Newitt et al., "Liquid Entrainment - 1. The Mechanism of Drop Formation from Gas or Vapor Bubbles", Trans. Instn. Chem. Engrs. 32, (1954), p. 244

(41) M. Tomaides, K.T. Whitby, "Generation of Aerosols by Bursting of Single Bubbles", in: B.Y.H.Liu (Ed.) "Fine Particles", Academic Press, N.Y., (1975)

(42) J.A. Day "Production of Droplets and Salt Nuclei by the Bursting of Air-Bubble Films", Quart. J. Roy. Meteor. Soc. 90, (1964), p. 72

(43) W. Hentschke, "Numerische Untersuchung über das Entstehen von Tropfen beim Zerplatzen von Gasblasen an Flüssigkeitsoberflächen", dissertation TU Clausthal, FRG, (1975)

(44) V.G. Gleim et al., "Drop Entrainment during Microbubbling", Zh. Prikl. Khim. (Leningrad) 43, (1970), p. 337

(45) N. Mitsuishi et al., "Studies on Liquid Entrainment", AEC-tr-4225

(46) S. Hayami, Y. Toba, "Drop Production by Bursting of Air Bubbles on the Sea Surface", J. Ocean. Soc. Japan 14, (1958), p. 145

(47) A.M. Rozen et al. "Entrainment of Moisture at Small Distance from a Bubbling Surface", Soviet Physics Doklady 19, (1974), No. 6, p. 338

(48) O. Preining et al., "The Size Distribution of Aerosols Produced by Air Blast Nebulization", J. Coll. Interf. Sci. 23, (1967), p. 458

(49) V.G. Gleim, "General Theory of the Carry-Over of Liquid from Boiling Solutions", J.Appl. Chem. USSR 28 (1955) no. 1,p.9

(50) F. Baumgärtner et al., still unpublished work done in the years 1979-1981 on research grant no. 02 U 5260 of the Fed. Department of Research and Technology, FRG

(51) M. Coantic, "Mass transfer across the ocean-air-interface", Phys. Chem. Hydrodyn. 1, (1980), p. 249

(52) R. Chesselet et al., "Variations in ionic ratios between reference seawater and marine aerosols", J. Geophys. Res. 77, (1972), p. 5116

(53) C.S. Martens, "Ion Ratio, Variations with Particle Size in Puerto Rican Aerosols", J.Geophys.Res. 78 (1973) 8867

(54) F. MacIntyre, "Flow Patterns in Bursting Bubbles", J. Geophys. Res. 77, (1972), p. 5211

(55) F. MacIntyre, "The Top Millimeter of the Ocean", Scientific American 230, (1974), No. 5, p. 62

(56) D.C. Blanchard, L. Syzdek, "Mechanism for the Water-to-Air Transfer and Concentration of Bacteria", Science 170, (1970), p. 626

(57) D.C. Blanchard, L. Syzdek, "Concentration of Bacteria in Jet Drops from Bursting Bubbles", J. Geophys. Res. 77, (1972), p. 5087

(58) H.F. Bezdek, A.F. Carlucci, "Surface Concentration of Maritime Bacteria", Limnol. Oceanograph. 17 (1972) no.4,p.566

(59) I. Kataoka, M. Ishii, "Mechanistic Modelling and Correlations for Pool-Entrainment Phenomenon", ANL-83-37, NUREG/CR-3304, (1983)

(60) H.J. Dorst, "Airborne Release of Particles Involved in the Evaporation of Radioactive Liquids", Jahrestagung Kerntechnik, Mannheim, (1982), poster session

(61) H.J. Dorst, NUKEM GmbH, private communication (1984)

(62) M. Fischer, Kraftwerk-Union, private communication (1984)

(63) W. Schütz, KfK, private communication (1984)

(64) B.J. Mason, "The Physics of Clouds" 2nd Ed., Clarendon Press, Oxford (1971)

(65) H. Bunz, et al., "NAUA Mod 4 , A Code for Calculating Aerosol Behaviour in LWR Core Melt Accidents, Code Description and Users Manual", KFK 3554, (1983)